

AD-A102 848

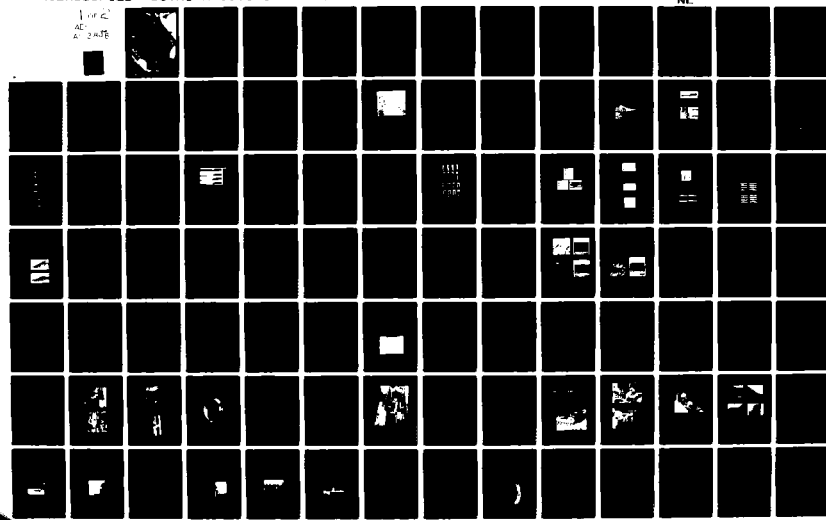
IIT RESEARCH INST CHICAGO IL
INTERNAL SHEAR FORGING PROCESSES FOR MISSILE PRIMARY STRUCTURES--ETC(U)
JUL 81 S RAJAGOPAL, S KALPAKJIAN

DAAK40-78-C-0264

NI

UNCLASSIFIED IITRI-M06013-33

F/6 20/11



ADA102848

LEVEL

iITRI

REPORT NO. IITRI-M68013-33

6 INTERNAL SHEAR FORGING

10

S. RAJAGOPAL
S. KALPAKJIAN

DTIC
ELECTED
AUG 14 1981

Final rept. 27 Sep 78-31 Mar 81
IIT RESEARCH INSTITUTE

IIT RESEARCH INSTITUTE

CHICAGO, ILLINOIS

15 DAAK40-98-C-9264

**U.S. ARMY MISSILE COMMAND
REDSTONE ARSENAL, ALABAMA**

20 JUL 81

2120

81

DISTRIBUTION STATEMENT A

Approved for public release

Distribution Unlimited

DC FILE COPY

175350 818 14019

UNCLASSIFIED

SECURITY CLASSIFICATION OF THIS PAGE (When Data Entered)

REPORT DOCUMENTATION PAGE		READ INSTRUCTIONS BEFORE COMPLETING FORM
1 REPORT NUMBER	2 GOVT ACCESSION NO	3 RECIPIENT'S CATALOG NUMBER
AD-A102 848		
4 TITLE (and Subtitle) Internal Shear Forging Processes for Missile Primary Structures		5 TYPE OF REPORT & PERIOD COVERED Final Report 9/27/78-3/31/81
7 AUTHOR(s) S. Rajagopal S. Kalpakjian		6 PERFORMING ORG. REPORT NUMBER IITRI-M06013-33
9 PERFORMING ORGANIZATION NAME AND ADDRESS IIT Research Institute ✓ 10 West 35th Street Chicago, IL 60616		8 CONTRACT OR GRANT NUMBER(s) DAAK40-78-C-0264
11 CONTROLLING OFFICE NAME AND ADDRESS U.S. Army Missile Command DRSMI-RLM Redstone Arsenal, AL 35898		10 PROGRAM ELEMENT PROJECT, TASK AREA & WORK UNIT NUMBERS MMT Project No. R783204(2597)
14 MONITORING AGENCY NAME & ADDRESS (if different from Controlling Office)		12 REPORT DATE 7/20/81
		13 NUMBER OF PAGES 109
		15 SECURITY CLASS (of this report) Unclassified
		16a DECLASSIFICATION/DOWNGRADING SCHEDULE
16 DISTRIBUTION STATEMENT (of this Report) Approved for public release; distribution unlimited		
17 DISTRIBUTION STATEMENT (of the abstract entered in Block 20, if different from Report)		
18 SUPPLEMENTARY NOTES		
19 KEY WORDS (Continue on reverse side if necessary and identify by block number) Internal shear forging Primary missile structures Shear spinning Thermomechanical treatment Near net shape processing Aluminum alloy 2014		
20 ABSTRACT (Continue on reverse side if necessary and identify by block number) Technology was established for combining thermomechanical treatment (TMT) with internal shear forging in the manufacture of 2014 aluminum alloy subshells with integral internal ribs. These structures are currently fabricated from 2014-T6 sheet and plate stock by welding together the cylindrical outer skin of the subshell and a series of internal stiffening rings. The objective of the project was twofold: to enhance the properties and performance of these structures by means of TMT and		

DD FORM 1 JAN 73 EDITION OF 1 NOV 68 IS OBSOLETE

UNCLASSIFIED

SECURITY CLASSIFICATION OF THIS PAGE (When Data Entered)

UNCLASSIFIED

SECURITY CLASSIFICATION OF THIS PAGE(When Data Entered)

20. Abstract (Continued)

to achieve cost reductions over the current (fabricated) parts as a result of single-piece construction and near net shape processing.

Internal shear forging consists of deforming a cylindrical ring between a rotating external die and an internal roller to result in a thin-walled tube with internal ribs in the circumferential direction. This form of processing was conducted, in this project, on a heavy-duty engine lathe equipped with special-purpose tooling and supplemented with a heat-treating furnace for the thermal treatments. Several different TMT cycles were evaluated in terms of the resulting tensile properties. Production requirements and process economics were also analyzed in detail.

It was concluded that internal shear forging can successfully replace the current technology; that significant cost savings would accompany the implementation of the new technology; but that additional work is necessary to test these parts for residual stresses, fatigue strength, crack propagation, and stress corrosion resistance, before the process can be considered ready for production.

UNCLASSIFIED

SECURITY CLASSIFICATION OF THIS PAGE(When Data Entered)

FOREWORD

This Final Manufacturing Methods Report covers the work performed by IIT Research Institute under Contract No. DAAK40-78-C-0264 (MM&T Project R783204) from 27 September 1978 to 21 March 1981. It is published for technical information only and does not necessarily represent the recommendations, conclusions, or approval of the U.S. Army.

This contract was initiated to establish Internal Shear Forging Processes for Missile Primary Structures, and was conducted under the direction of Mr. John Honeycutt/DRSMI-RLM, U.S. Army Missile Command, Redstone Arsenal, Alabama. At IIT Research Institute, Mr. S. Rajagopal, Manager, Mechanical Systems and Design, was the principal investigator. Notable contributions were made by Mr. A. Chakravarthy, Mr. C. Hales, Mr. W. Mitchum, Mr. J. Oni, Mr. A. Omotosho, and Dr. S. Agarwal. Professor S. Kalpakjian of IIT served as consultant to the project team.

Rajagopal

S. Rajagopal, Manager
Mechanical Systems
and Design Section

Approved by:

Alan Howes

M. A. H. Howes, Director
Materials and Manufacturing
Technology Division

Accession No.	
NTIS Grade	<input checked="" type="checkbox"/>
NTIS Size	<input type="checkbox"/>
Unnumbered	<input type="checkbox"/>
Justification	
By	
Distribution	
Availability Dates	
Comments	

A

CONTENTS

	<u>Page</u>
FOREWORD	iii
1. INTRODUCTION	1
2. PROGRAM OBJECTIVES AND SCOPE	2
3. REVIEW OF INTERNAL SHEAR FORGING AND RELATED PROCESSES	5
3.1 The Basic Process of Shear Forging of Tubes	6
3.2 Typical Components Produced by the Shear Forging Process and Their Properties.	14
3.3 Theoretical and Experimental Studies in Shear Forging of Tubes.	17
3.3.1 Spinnability of Materials.	18
3.3.2 Material Flow and Resulting Dimensional Changes.	24
3.3.3 Forces in Shear Forging of Tubes	31
4. 2014 ALUMINUM ROLLING EXPERIMENTS.	36
4.1 Task Objectives	36
4.2 Starting Material	37
4.3 Rolling Experiments	41
4.4 Microstructural Observations.	47
4.5 Conclusions	52
5. TOOLING DESIGN AND FABRICATION	53
5.1 Shear Forging Machine	53
5.2 Basic Considerations in Tooling Design.	53
5.2.1 Die Construction	53
5.2.2 Roller Design for Shear Forging.	54
5.2.3 Design Parameters Affecting Surface Finish	55
5.3 Initial Tooling Design and Trials	57
5.4 Tooling Modifications	62
6. INTERNAL SHEAR FORGING OF SUBSHELLS.	66
6.1 Process Description	66
6.2 Metal Flow.	69
6.3 Shear Forging of 2014 Al and 2024 Al Subshells.	78
6.4 Thermomechanical Treatment of 2014 Al Subshells	81
6.5 Processing of Deliverable Subshells	93
6.5.1 Deliverable Items.	93
6.5.2 Residual Stresses.	94
6.5.3 Thin Rib Generation.	94

CONTENTS (continued)

	<u>Page</u>
7. PRODUCTION REQUIREMENTS AND COSTS.	97
7.1 Equipment and Tooling	97
7.2 Production Process Sequence	98
7.3 Standard Hours for Subshell Production.	98
7.3.1 Heat Treatment Station	99
7.3.2 Spinning Lathe Station	99
7.3.3 Machining Station.	101
7.3.4 Inspection Station	102
7.4 Subshell Production Cost for Internal Shear Forging vs. Current Process.	102
7.4.1 Production Cost--Internal Shear Forging.	103
7.4.2 Production Cost--Current Process	103
7.4.3 Return on Investment and Payback Period.	103
8. CONCLUSIONS AND RECOMMENDATIONS.	104
REFERENCES	105
DISTRIBUTION LIST.	108

TABLES

<u>Number</u>		<u>Page</u>
1	Mechanical Properties and Chemical Composition of As-Received 2014-T651 Aluminum Alloy Rolled Plate	38
2	Mechanical Properties of 2014-O Aluminum Alloy Plate Used as Starting Material in Rolling Experiments.	38
3	Rolling Experiments with 2014-O Aluminum Alloy with Different Lubricants.	44
4	Effect of Rolling Speed and Heat Treatment on Mechanical Properties of Aluminum Alloy 2014	45
5	Effect of Blank Temperature and Rolling Reduction on Mechanical Properties of Aluminum Alloy 2014.	46
6	Mechanical Properties of Internally Shear Forged Samples. . .	79
7	Surface Finish of Internally Shear Forged Parts	80
8	Tensile Properties of Internally Shear Forged 2014 Aluminum Alloy after Different Thermal-Mechanical Cycles	91
9	Effect of Final Aging Treatment on Tensile Properties of 2014 Aluminum Alloy	92

FIGURES

<u>Number</u>		<u>Page</u>
1	Subshell target geometry for internal shear forging	2
2	Program tasks and schedules	4
3	The shear forging process	6
4	Jet engine turbine drive shaft roll-formed from AMS 6415 alloy steel forged preform.	8
5	Rear compressor-case layout for flow turning.	8
6	HP9-4 motor case internally roll-extruded from preform.	9
7	Shape capability by shear forming cylinders from rings.	10
8	Forces on roller during internal shear forging.	11
9	Comparison of grid deformation, photomicrograph, and isohardness (Vickers) lines in shear forged copper tubing with 66% reduction, $\frac{1}{4}$ in. original thickness.	12
10	Longitudinal section through the wall of a cylindrical workpiece showing expansion of the unspun section	13
11	Distortion of shear forged parts ahead of the deformation zone.	13
12	Schematic diagram of workpiece deformations investigated in reference 33.	13
13	Internal and external roll extrusion with workpiece pulled through die-roller gap.	15
14	Internal roll extrusion of ribs using moving inner mandrel.	16
15	Test setup to subject tubes to continuously increasing wall reduction by shear forging	18
16	Sections of fractured samples from spinnability tests, indicating degree of forward reduction permissible for (A) 2024-T4 Al, (B) 6061-T6 Al, (C) annealed copper, and (D) mild steel.	19
17	Maximum reduction in shear forging of various materials as a function of tensile reduction of area	20
18	Chevron cracking caused by small reductions and large die angles in extrusion, drawing, and shear forging, shown here for cold tube extrusion.	23
19	Buildup in various stages of shear forging and influence of roller nose radius on buildup formation.	25
20	Stages in shear forging with three different methods using the same roller	26
21	Influence of skew angle on buildup formation.	26
22	Influence of contact angle α of roller on buildup formation .	26

FIGURES (continued)

<u>Number</u>		<u>Page</u>
23	Influence of original wall thickness on buildup formation.	27
24	Comparison of calculated angles of buildup with actual buildup profiles in forward shear forging.	27
25	Influence of roller angle, feed rate, and reduction on buildup and distortion ahead of roller	28
26	Roller geometry and nomenclature	29
27	Section through workpiece showing material flow.	30
28	Force coefficients in forward and backward shear forging	32
29	Force factors vs. thickness reduction in backward shear forging.	33
30	Force factors vs. thickness reduction in forward shear forging.	33
31	Contact geometry in external and internal shear forging of tubes	35
32	Precipitate phases in 2014-T651 as-received plate.	39
33	Finely dispersed precipitate phase observed after annealing (prior to rolling)	40
34	Reduction sequence for rolling of 2014-0 aluminum alloy.	42
35	Summary of rolling experiments for 2014 aluminum alloy	43
36	Photomicrographs, (a) optical and (b) SEM, of as-rolled structure after 95 percent reduction by rolling at 149°C	48
37	Photomicrographs, (a) optical and (b) SEM, of as-rolled structure after 95 percent reduction by rolling at 316°C	50
38	Optical photomicrographs of samples rolled to 95% reduction, solution treated and naturally aged to the T4 condition.	51
39	Initial tooling design for internal shear forging.	58
40	Experimental setup for internal shear forging.	59
41	Shear forging roller unit.	59
42	Side view of tooling for internal shear forging.	60
43	Initial tooling setup for internal shear forging	60
44	2014 aluminum alloy ring, partially deformed by internal shear forging.	61
45	Improved tooling design for internal shear forging	63

FIGURES (continued)

<u>Number</u>		<u>Page</u>
46	Modified tooling for internal shear forging, assembled in LeBlond 2516 engine lathe	64
47	Modified rollers for internal shear forging.	65
48	Process elements in internal shear forging of 2014 Al subshells.	66
49	Internal shear forging of aluminum rings into thin-walled, internally ribbed tubes.	67
50	Graphite spray lubrication during initial warm deformation in internal shear forging.	67
51	Adjusting screw being turned for rib forging	68
52	Intermediate tube wrapped in aluminum foil (to prevent heating) and loaded in furnace for solution treatment.	68
53	Thermomechanically treated, internally ribbed tube being removed from the die	69
54	Low-magnification photomicrographs showing metal flow in internal shear forging	70
55	Fold produced due to inhomogeneous deformation, shown schematically (a) and on an actual part (b).	72
56	Lamination defect, caused on the ID surface during rib forging by foldover of buildup from previous passes, shown schematically (a) and on an actual part (b).	73
57	Cracking of wall OD from secondary tensile stresses due to high radial feed, low temperature, inadequate roller clearance, and rough machining marks on preform OD, shown schematically (a) and on an actual part (b).	75
58	Buckling of thick wall ahead of roller and thin wall behind roller due to heavy reduction and feed rate in final pass, shown schematically (a) and on an actual part (b)	76
59	Void observed in thin wall in one case, attributable to hard inclusion or entrapment of wear debris in final pass, shown schematically (a) and on an actual part (b).	77
60	Inside surface finish of part produced by ISF/RF	80
61	Thermomechanical treatment (TMT) cycles evaluated during internal shear forging of 2014 aluminum alloy.	83
62	Optical photomicrographs of 2014-0 aluminum specimen prior to internal shear forging.	84

FIGURES (continued)

<u>Number</u>		<u>Page</u>
63	Optical photomicrographs of internally shear forged 2014 aluminum specimen after cycle 1.	85
64	Optical photomicrographs of internally shear forged 2014 aluminum specimen after cycle 2.	86
65	Optical photomicrographs of internally shear forged 2014 aluminum specimen after cycle 3.	87
66	Optical photomicrographs of internally shear forged 2014 aluminum specimen after cycle 4.	88
67	Optical photomicrographs of internally shear forged 2014 aluminum specimen after cycle 5.	89
68	Optical photomicrographs of internally shear forged 2014 aluminum specimen after cycle 6.	90
69	Deliverable subshells, internally shear forged with thermomechanical treatment	93
70	Residual stresses from internal shear forging of preaged material	95
71	Observation of residual stresses by cutting a thermo-mechanically processed subshell.	96

1. INTRODUCTION

Missile primary structures are currently fabricated from 2014 aluminum alloy sheet and plate stock by welding together the cylindrical outer skin of the structure and a series of internal stiffening rings. Cost reductions are sought for large production quantities by implementing internal shear forging to produce these structures in monolithic construction. An additional benefit is the possibility of enhancing structural performance by incorporating thermomechanical treatments (TMT) into the internal shear forging process for these structures.

Internal shear forging consists of deforming a cylindrical ring between a rotating external die and an internal roller, resulting in a thin-walled tube with integral internal ribs. It is fairly well established as a production process for axisymmetric components and is known by a variety of names including internal tube spinning and internal roll extrusion.

The objective of this program was to establish the internal shear forging process for missile primary structures featuring thermomechanical treatment. For aluminum alloys, TMT typically involves introducing cold work into the precipitation-hardening cycle which results, in many cases, in improved tensile properties, fatigue strength, fracture toughness, and stress corrosion resistance.

The work performed on this program and covered in this report included tooling design and fabrication, an exploratory study of basic parameters, internal shear forging experiments, processing of deliverable parts with thermomechanical treatment, tensile property determination, and an economic analysis involving considerations of production requirements and costs for internal shear forging.

2. PROGRAM OBJECTIVES AND SCOPE

The target component for this program (Figure 1) was a simplified subscale version of a missile primary structure and is referred to hereafter as the "subshell." The objective of the program was to establish tooling requirements and manufacturing procedures to shear forge the subshell with thermomechanical treatment during processing.

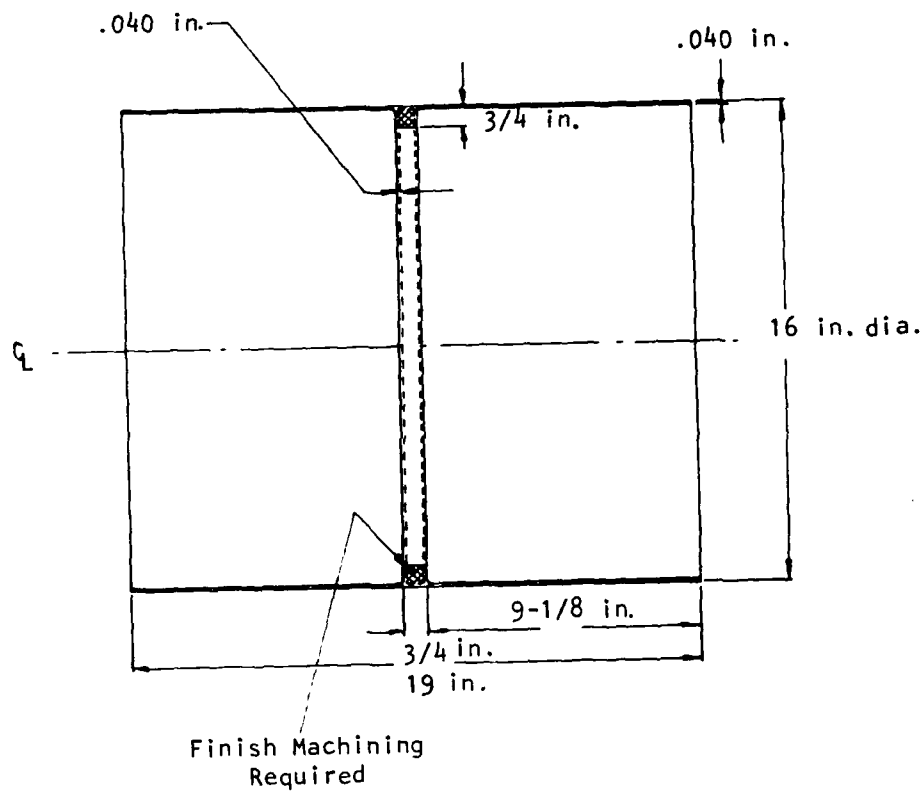


Figure 1. Subshell target geometry for internal shear forging.

The program was organized in two phases. Phase I (Basic Effort) involved rolling experiments with 2014 aluminum, and tooling design and fabrication for internal shear forging. In Phase II (Option 1), tooling trials were made, followed by tooling modifications, final trials,

evaluation of various TMT cycles by tensile property determination, internal shear forging of deliverable parts, and cost analysis for manufacture.

Figure 2 shows the tasks and schedules for both phases of the program.

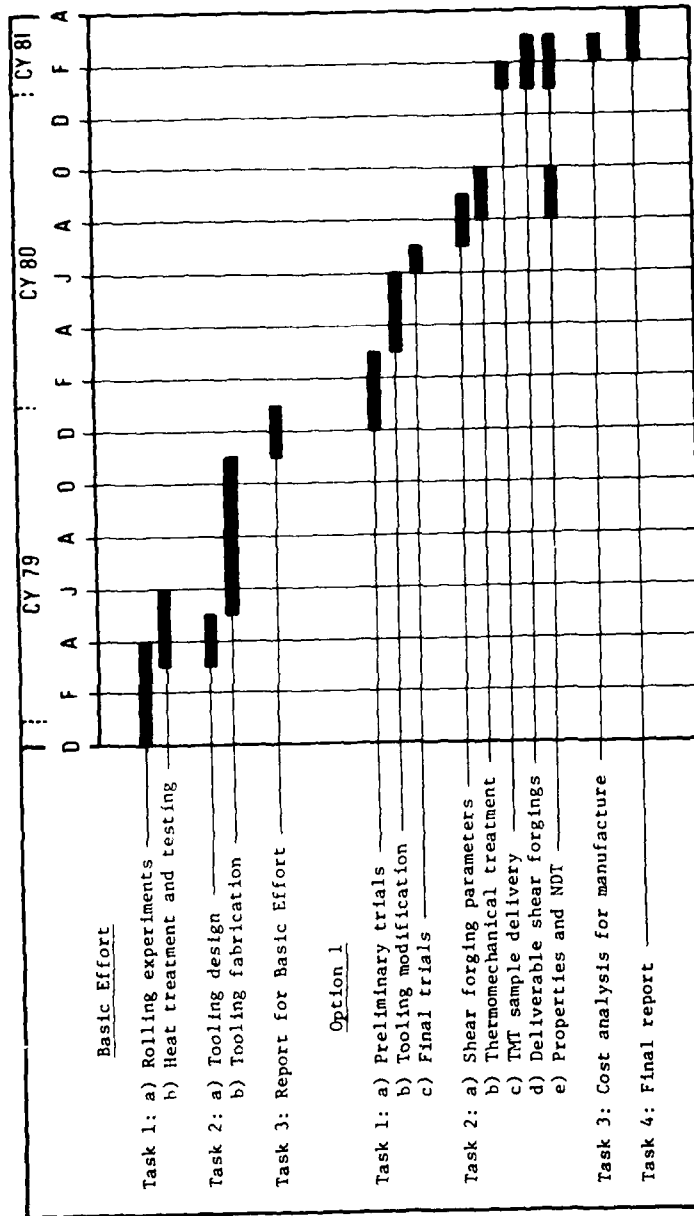


Figure 2. Program tasks and schedules.

3. REVIEW OF INTERNAL SHEAR FORGING AND RELATED PROCESSES

This section outlines the state-of-the-art in shear forging of tubes, both external and internal, whereby the original tubular blank is subjected to wall thickness variations along its length while maintaining rotational symmetry. The process is known in industry by a variety of other names such as shear forming, tube spinning, flow turning, spin forging, rotary extrusion, roll extrusion, flow forming, hydrospinning, rotoforming, and floturning. Although all these terms describe the basic process that is common to all spun parts, there are some differences among them. These differences generally pertain to the type of rollers, mandrels, and machines used in making these parts. In this report, the process will be referred to as shear forging.

The shear forging process is quite versatile in view of the fact that a great variety of tubular parts can be manufactured with basically the same tooling. This is done by controlling the path of the rollers during their longitudinal travel along the length of the workpiece and by controlling roller geometry and reduction in thickness. Typical components are pressure vessels, automotive, and rocket and missile parts. The process is suitable not only for prototype or low production runs, but also for high-production runs on automated equipment. Shear forging can be quite economical due to relatively low tooling costs, material utilization, and the ease with which design changes can be made.

Depending on the strength and ductility of the workpiece material and the capacity of the machine, the shear forging process can be carried out either at room temperature or at elevated temperatures. The resulting properties of the product will, of course, depend on the particular material and process parameters, such as reduction and temperature. In general, the mechanical properties are enhanced, thus making the process attractive for strong but lightweight designs. Various general surveys of the shear forging process can be found in the literature, more recent ones being given in References 1 through 4.

In view of its many advantages, this process has been studied quite extensively during the past thirty years or so. These studies have ranged from the most analytical to the most applied aspects, the latter including basically developmental work in tooling and process control in order to obtain components of certain specified geometries. Contributions to the understanding of the process have been concerned with force and power requirements, spinnability of materials, material flow, surface deformations at the roller-workpiece interface, properties of spun parts, and how these factors are related to process parameters and original material properties. Such understanding is essential in order to make full use of the capabilities of this process and to aid in the design of components to be spun. Although the majority of these studies have been on external shear forging, much of the knowledge gained should be equally applicable to internal shear forging.

3.1 THE BASIC PROCESS OF SHEAR FORGING OF TUBES

The basic process of shear forging is shown in Figure 3, both for external and for internal spinning. The original tubular blank is placed on the mandrel (in the case of internal shear forging, inside the die), and a roller of a certain geometry travels axially, reducing the thickness of the blank.

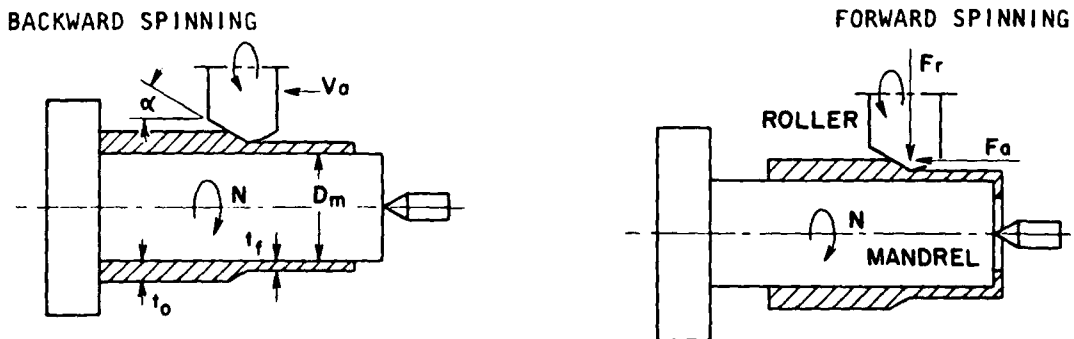


Figure 3. The shear forging process (also known as shear forming, tube spinning, flow turning, spin forging, rotary extrusion, roll extrusion, flow forming, hydrospinning, rotoforming, and floturning).

It can be readily recognized that there are a number of independent variables in this basic process. These are listed below.

a) Mandrel Diameter and rpm

It can be seen that the mandrel does not necessarily have to be of constant diameter along its length, and that a variety of parts can be shear forged with shaped mandrels, provided that the mandrels have rotational symmetry, Figures 4-7.

b) Roller Size, Geometry, and Orientation

A great variety of roller geometries have been developed over the years. The contact geometry between the roller and the workpiece is important and could play a critical role in the successful operation of the process.

Whereas there is a maximum limit to roller diameter in internal shear forging, there is no such limitation for external shear forging. It is obvious, of course, that as the roller diameter increases, the contact area between roller and workpiece increases; this will then influence the magnitude of the forces involved, as will be described later.

The power input into this process can be either through the mandrel (such as by placing it on the headstock of a lathe) or through the roller (by powering the shaft on which the roller is placed).

c) Feed

The distance traveled by the roller per revolution of the mandrel is referred to as feed. It is an important parameter as it has influence on surface finish and dimensional control of the final diameter of the shear forged product. In situations where more than one roller is used, the effective feed rate for each roller will be less.

d) Reduction per Pass

Because of its great influence on a number of parameters, reduction per pass has been studied extensively. Its effects depend not only on other variables (such as roller geometry), but also on the mechanical properties of the workpiece material.

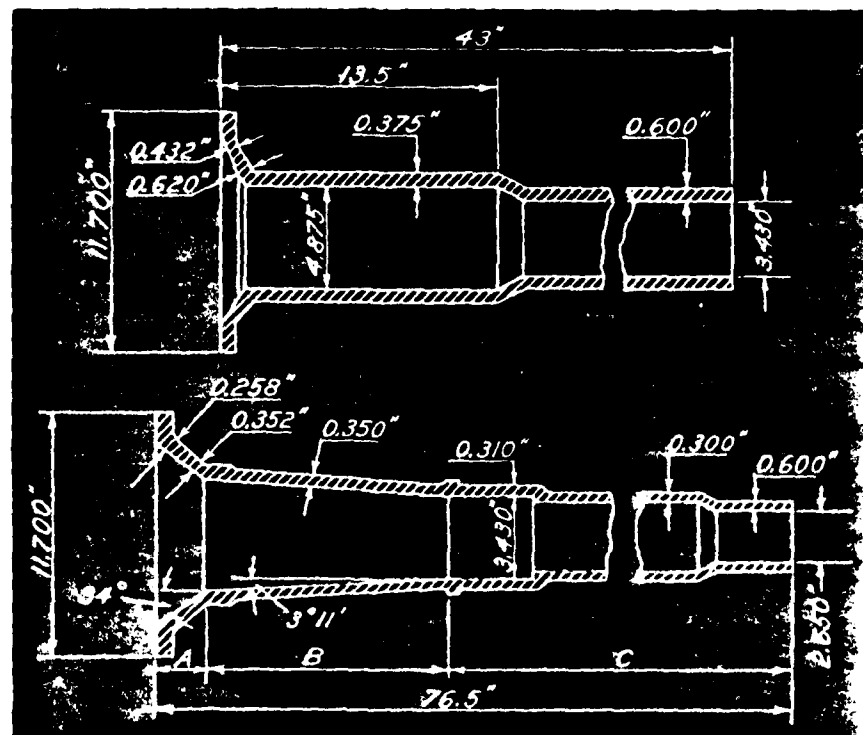


Figure 4. Jet engine turbine drive shaft (bottom) roll-formed from AMS 6415 alloy steel forged preform (top).⁷

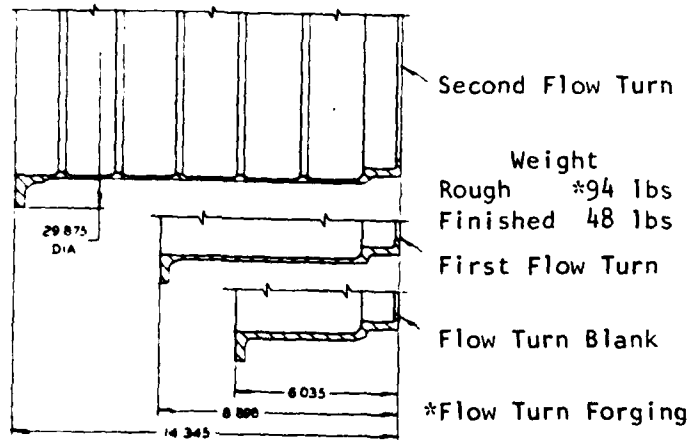


Figure 5. Rear compressor-case layout for flow turning.⁸
(All dimensions in inches.)

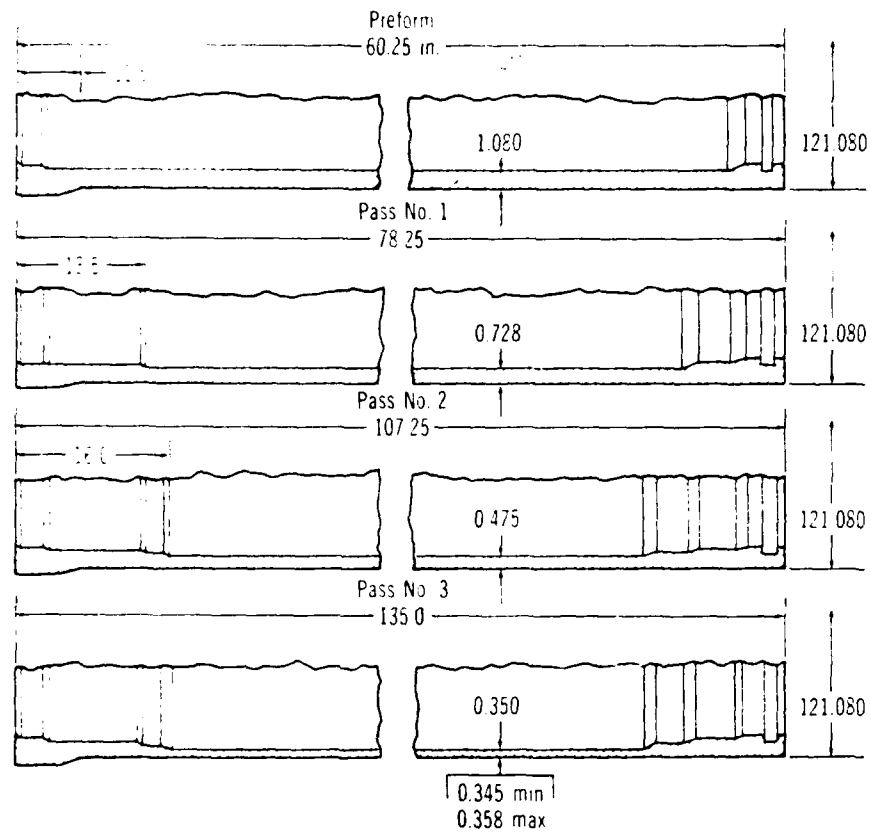


Figure 6. HP9-4 motor case (bottom) internally roll-extruded from preform (top).¹² (All dimensions in inches.)

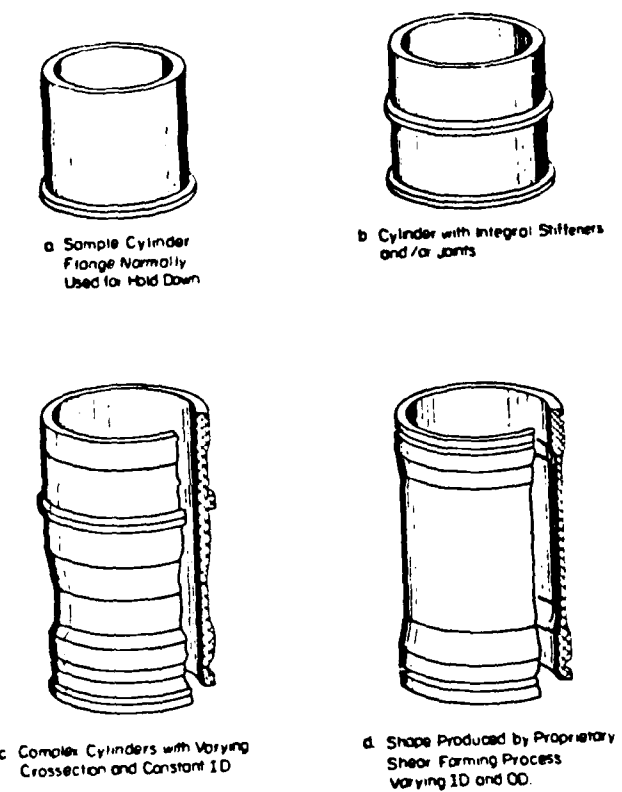


Figure 7. Shape capability by shear forming cylinders from rings.³

e) Workpiece Material

The properties relevant to workpiece materials are mechanical (strength and ductility), metallurgical (role of impurities, response to thermomechanical treatment), and physical (specific heat, and coefficients of thermal conductivity and expansion). The interrelationship of these properties and other variables of the process is quite complex. Some details will be discussed later in this section.

The foregoing independent variables will have influence on the following dependent variables of the process:

a) Forces. As can be seen in Figure 8, there are three principal force components in shear forging of tubes. These are axial, radial, and tangential. In calculating the individual power components involved with each of these forces, it can be shown that the most significant force is the tangential force, F_t , which supplies the torque to the system. The role of the axial force, F_a , is rather small by virtue of the fact that the axial distance traveled by this force is quite small. The radial force, of course, does not contribute to the power consumed in the process.

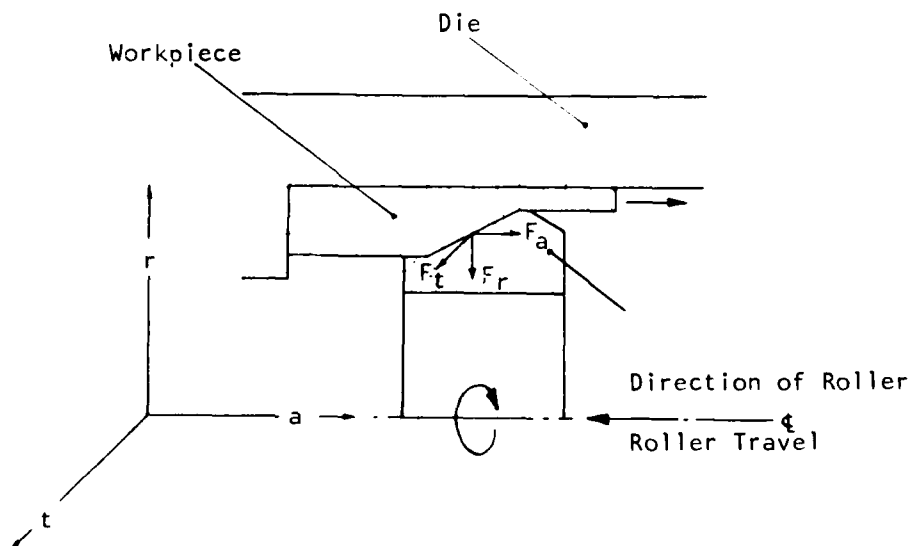


Figure 8. Forces on roller during internal shear forging. (F_a , F_r , and F_t are associated with compressive stresses in the unspun region of the workpiece in the axial, radial, and tangential directions, respectively).

Knowledge of these forces is essential not only for determining the power consumption, but also for the design of machines--particularly when high rigidity is required for better dimensional control of the process.

b) Material Flow. There are two aspects to this parameter. One is the bulk flow of the material in the deformation zone, Figure 9, and the other is the distortion, ahead of the roller, of both internal and external surfaces of the tube being shear forged, Figures 10 to 12.

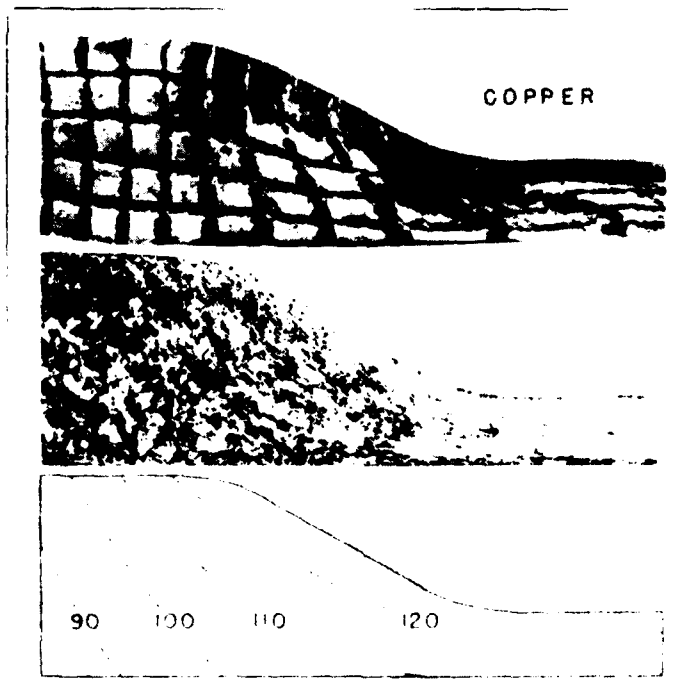


Figure 9. Comparison of grid deformation, photomicrograph, and isohardness (Vickers) lines in shear forged copper tubing with 66 percent reduction, $\frac{1}{4}$ in. original wall thickness.²¹

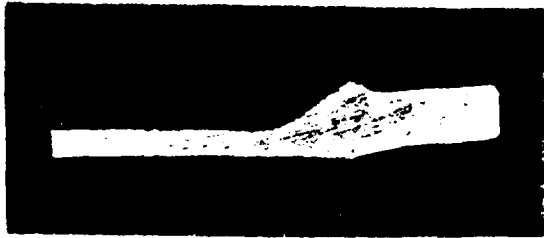


Figure 10. Longitudinal section through the wall of a cylindrical workpiece showing expansion of the unspun section. Original wall thickness = 6 mm material = 0.15 percent C steel.³³

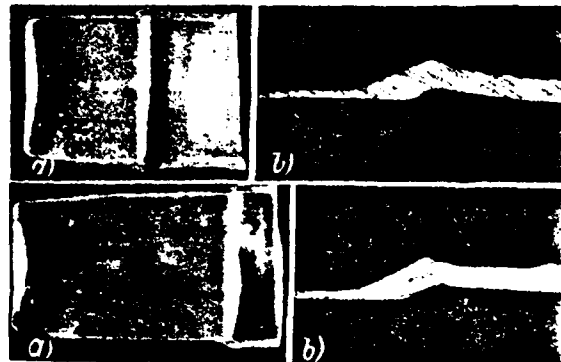


Figure 11. Distortion of shear forged parts ahead of deformation zone. (a) Cup shear forged to (top) half and (bottom) almost its full length; (b) transition between shear forged wall and original wall.²⁴

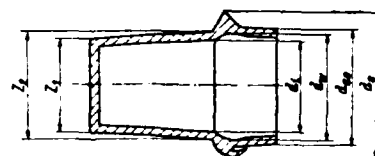


Figure 12. Schematic diagram of workpiece deformations investigated in reference 33.

Bulk flow characteristics determine the final properties of the tube (including the role played in thermomechanical treatment), and can also play a role in defect formation in the product. Surface flow is important for residual stresses and in dimensional control of all surfaces of the workpiece, although it can also influence the quality of the product at or near the surfaces. Because they can change the contact area and geometry at the roller-workpiece interface, surface flow characteristics also influence forces.

3.2 TYPICAL COMPONENTS PRODUCED BY THE SHEAR FORGING PROCESS AND THEIR PROPERTIES

A great variety of components have been produced by the shear forging process of conical, curvilinear, and tubular geometries. In this section, only tubular shapes will be discussed. In addition to simple, constant wall thickness tubes, both external and internal geometries and ribs can be obtained, as shown in Figures 13 and 14, and earlier in Figures 5 to 7.

External shear forging has been used, thus far, more commonly than internal shear forging, as reflected in the technical literature. References 1-15 pertain to external and 16-17 to internal shear forging (roll extrusion).

Whereas in external shear forging the power to the system is generally supplied through the mandrel (with idling rollers), in roll extrusion the power is often supplied through the rollers. The part is pulled through stationary rollers by grippers (Figure 13) or reduced in wall thickness by a moving internal roller (Figure 14).

As can be seen from the illustrations in the literature, typical parts made by these processes are cylindrical shapes of a large variety of materials, with or without external and internal ribs and flanges. This process has been proven to be more economical than other processes to manufacture these same parts. Thus, the process has had wide applications in aerospace, military, and nuclear fields, in addition to a wide range of applications for commercial products.

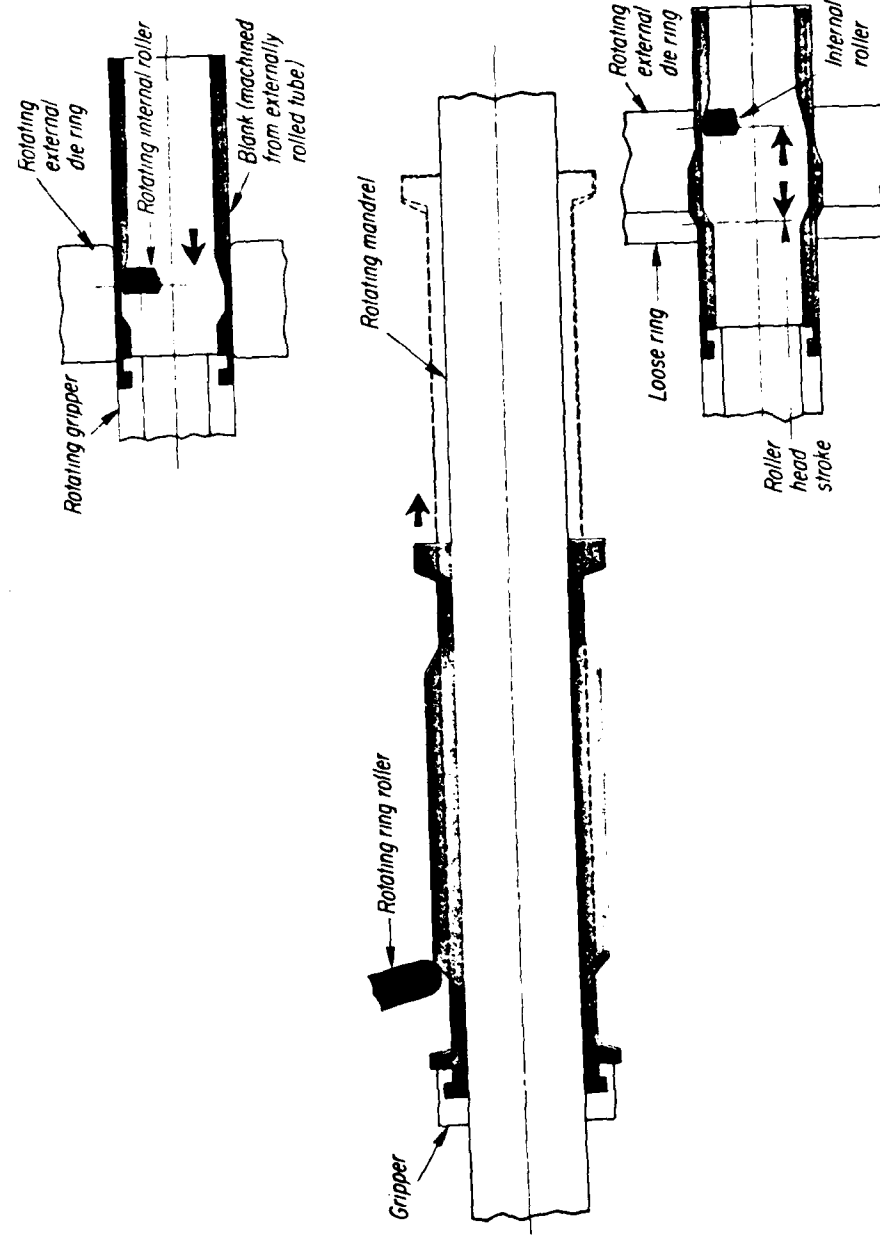
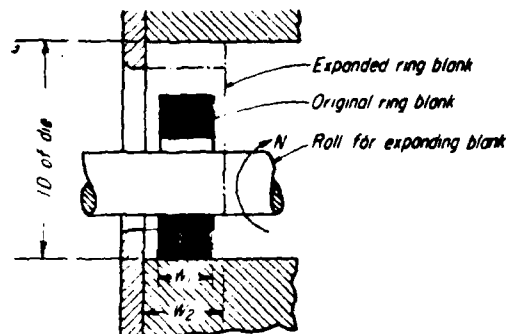
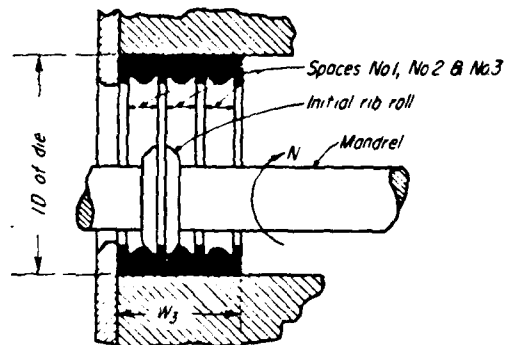


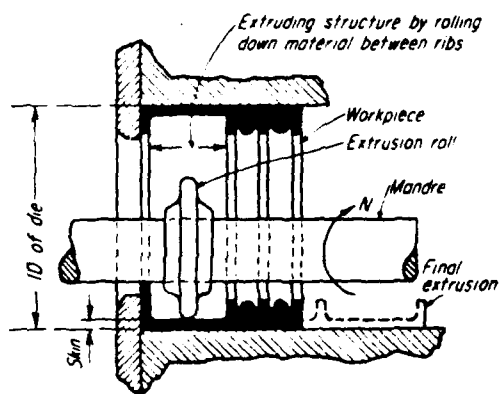
Figure 13. Internal and external roll extrusion with workpiece pulled through die-roller gap.¹⁷



Expand Original Blank Against ID of die



Initial Rolling of Rib



Axial Extrusion of Structure

Figure 14. Internal roll extrusion of ribs using moving inner mandrel.¹⁶

In addition to reducing costs and material savings, the process enhances the mechanical properties of the material as shown in the present study and also in the technical literature.^{3,18,19} The increase in properties will, of course, depend on the workpiece material, reduction, and temperature. As expected, strength and hardness increase with a corresponding decrease in ductility. These properties can then be altered with post-processing heat treatment, such as stress relieving and annealing.

A significant aspect in property enhancement is the thermomechanical treatment (ausforming) before and during the shear forging cycle. In one study on external shear forging of low alloy steel tubes, it was shown that thermomechanical treatments produced tubes with very high yield strength combined with good ductility.²⁰

As it has been shown in the present study, such processing is also applicable to the internal shear forging of 2014 aluminum tubes with possible enhancement of their mechanical properties.

3.3 THEORETICAL AND EXPERIMENTAL STUDIES IN SHEAR FORGING OF TUBES

In view of its technological significance, the shear forging process has been the subject of studies for the past three decades or so. These studies have ranged from the most analytical to the research and development type work in various industrial organizations. The principal focus on these studies is mainly toward establishing relationships between material and process variables and such parameters as forces and spinability of materials.

A general survey of the more technical studies on the subject is given in Reference 21. Much of the technical literature pertains to shear forging of conical shapes. The earliest systematic study of tubular shapes appears to have been done in 1961.²² Since then, a number of publications have appeared on various aspects of shear forging of tubes.²³⁻³⁹ None of these studies pertain to internal shear forging. It is expected, however, that many of the quantitative relationships obtained for external shear forging would also be applicable to internal shear forging.

The studies conducted thus far have been directed toward an understanding of the following parameters: spinnability of materials, material flow and resulting dimensional changes, and force and power requirements as a function of process parameters and material properties. These will now be discussed in terms of their engineering relevance.

3.3.1 Spinnability of Materials

Spinnability of materials is defined as the maximum reduction per pass that the material can undergo before failure takes place. It is, of course, desirable to study this process and predict, by analytical or empirical means, whether or not a given workpiece of certain dimensions and properties will withstand the stresses imposed upon it. From Figure 3, it will be noted that in forward shear forging the spun section is in tension, and in backward shear forging the unspun section is in compression. Thus, the failure modes will be in tension and by buckling, respectively.

It appears that the only systematic study of this subject is that given in Reference 26. With a test setup as shown in Figure 15, a number

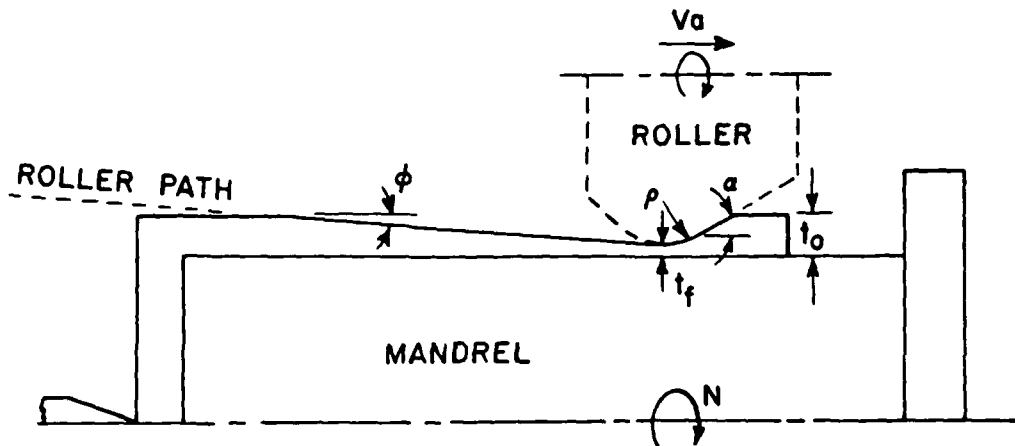


Figure 15. Test setup to subject tubes to continuously increasing wall reduction by shear forging.²⁶

of metals were spun with increasing reduction in thickness until tensile failure (or failure in the deformation zone) occurred. Sections of these metals illustrating failure are shown in Figure 16. Additional studies

were conducted to determine the influence, if any, of process variables such as feed, roller corner radius, and roller angle (equivalent to die angle) on this maximum reduction per pass.



Figure 16. Sections of fractured samples from spinnability tests, indicating degree of forward reduction permissible for (A) 2024-T4 Al, (B) 6061-T6 Al, (C) annealed copper, (D) mild steel.

Attempts were then made to establish a quantitative relationship between spinnability and material properties. The results indicated that the property that was most relevant was the tensile reduction of area of the original tube material in the longitudinal direction, Figure 17. It is interesting to note that, up to a tensile reduction in area of about 50%, spinnability was more or less a direct function of the ductility of the material. The material failed because of lack of ductility as required by the thickness variation. Above 50%, a plateau was reached, indicating that failure was due to tensile stresses in the spun section of the tube; in this case the ductility of the tube material is of no primary significance. (This analogy is the same as that used in determining maximum theoretical reduction per pass in wire, rod, or tube drawing.)

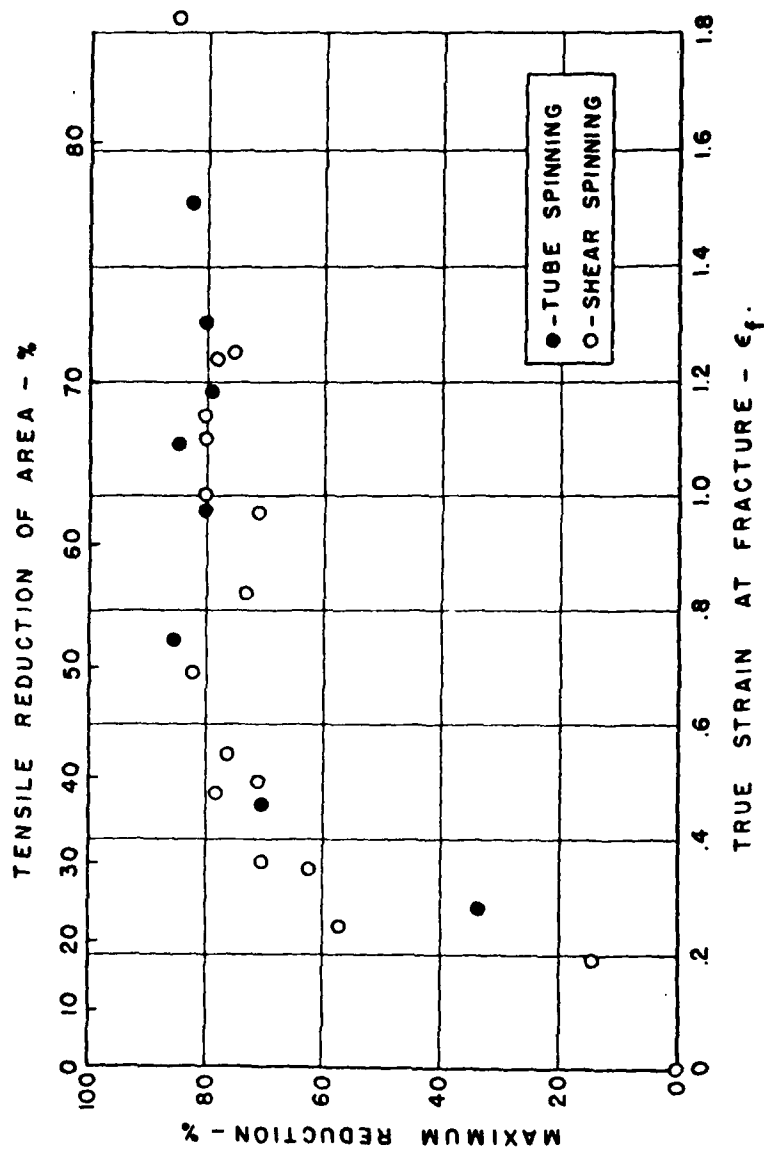


Figure 17. Maximum reduction in shear forging of various materials as a function of tensile reduction of area.²⁶

In experiments with mild steel and copper, it was shown that the maximum reduction per pass decreased with increasing feed. This decrease could be attributed to an increase in the axial force with increasing feed, thus increasing the stresses in the spun section of the tube. Maximum reduction per pass decreased slightly with increasing roller corner radius, while roller angle had no influence on maximum reduction.

In additional experiments, tubes were reduced in thickness by spinning, in order to subject them to different degrees of cold work. These tubes were then shear forged in the same setup as Figure 15 to determine the maximum reduction per pass. The amount of prior cold work did not have any significant influence on the maximum reduction. This means that in multiple-pass operations the same maximum safe reduction may be employed continuously at each pass.

Although these studies have not been extended to internal shear forging, there is no particular reason to believe that the external shear forging results obtained would not be applicable. The two processes are essentially the same; the wall-thickness-to-mandrel (die)-diameter ratio is essentially the same, and the deformation zone and the stresses to which the material is subjected are also the same. The only major difference is that, under similar conditions, the contact area between the roller and the workpiece is larger in internal than in external shear forging.

As far as backward shear forging is concerned (a process which has a wider application because of the ease with which it can be carried out), spinnability becomes somewhat difficult to determine because: (a) As the thickness reduction per pass increases, reverse buildup under and ahead of the roller takes place, (b) buckling of the unspun section of the tube takes place as the longitudinal spinning forces increase due to increasing reduction, and (c) the buckling will depend on the length of the unspun tube section.

It would appear, however, that for both the external and internal case, the ductility of the workpiece material will be important. This is because the material is subjected to a reduction in thickness and it

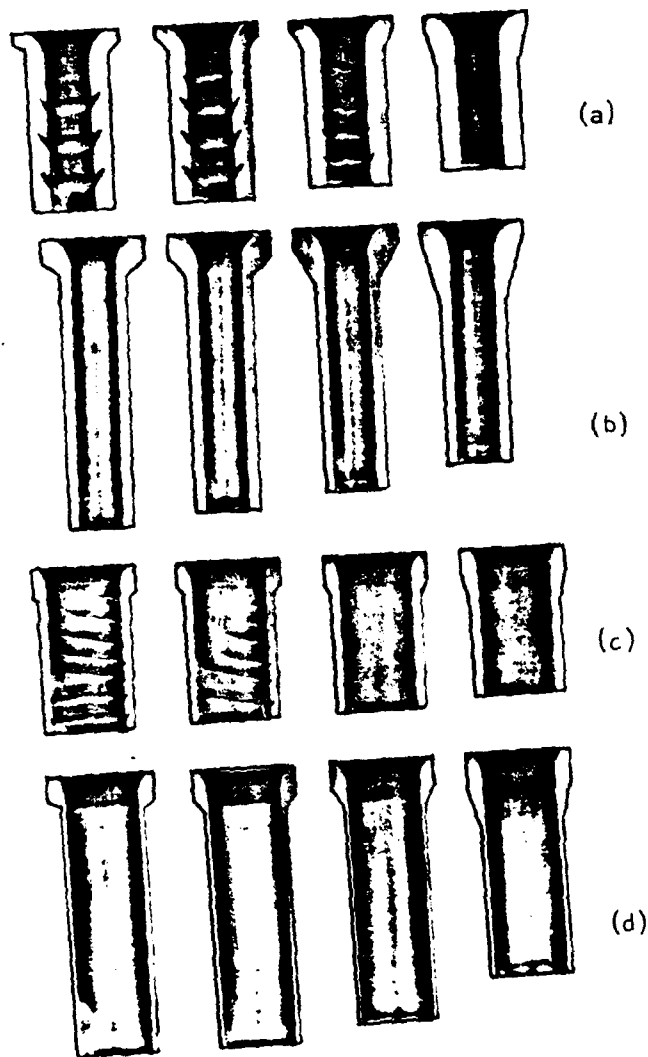
must have the capacity of undergoing large strains to failure. It should be pointed out that, as shown in numerous studies, ductility is very much a function of the state of stress and that a compressive environment is desirable for enhanced ductility.

From this point of view, it would appear that internal backward shear forging is a particularly desirable situation.

The discussion, thus far, has been concerned with maximum reduction per pass. It should be pointed out that light reductions can also have adverse effects on the spun product. This is due to the fact that light reductions will deform mainly the surface layers of the tube with little deformation of the bulk of the material under the roller.

Whereas light reductions in shear forging may be desirable for work-hardening the surface layers of the product (just as in shot peening, with beneficial increase in the fatigue life), they can have a strong adverse effect on the product quality.^{29,30} This is due to the fact that, with light reductions, the plastic zone under the roller does not fully penetrate the thickness of the tube. This subsequently generates a hydrostatic tensile stress component which can cause cracks on the mandrel side of the tube wall (Figure 18). The mechanism is the same as that obtained in drawing and extrusion of solid tubular parts, the fracture being called by a variety of names such as centerburst, chevron, arrowhead, and cuppy core. The generation of these cracks is further accelerated by the presence of impurities and inclusions, particularly if they are hard.

To avoid such fractures in shear forging, two important parameters have to be controlled. One is the percent reduction. Under otherwise identical conditions, higher reductions will reduce or eliminate fracture by assuring that the plastic zone penetrates the thickness of the tube. The other parameter is the roller geometry. The smaller the roller angle (equivalent to the die angle in drawing), the larger and deeper the deformation zone. Furthermore, the radius between the roller angle and its relief angle is important, particularly at small reductions on thin-walled tubes. This is because the larger this radius, the smaller the effective roller angle.



Cracking resulting from two-stage cold extrusion.
 Various die angles: from left to right, 120° , 90° , 60° , 30° .
 (a) First stage 1.23, second stage 1.8
 (b) First stage 1.23, second stage 3.6
 (c) First stage 2.0, second stage 1.8
 (d) First stage 2.0, second stage 3.6

Figure 18. Chevron cracking caused by small reduction and large die angles in extrusion, drawing, and shear forging, shown above for cold tube extrusion.³⁰

3.3.2 Material Flow and Resulting Dimensional Changes

In addition to the bulk deformation of the material between the roller and the mandrel, deformation of the outer and inner surfaces of the tube is important. This aspect of shear forging of tubes has been the subject of study ever since the systematic work by Thomasett²² in 1961, although many relevant observations had been made prior to that time in research studies by commercial organizations.

This subject falls into two categories. One is the diametral control of the tube, and the other is the dimensional control of the surfaces of the tube, particularly in generating ribs and flanges of prescribed geometries.

In external shear forging, two important parameters in diametral control are the feed and the roller geometry. Diametral growth is akin to ring rolling and also to spread in plate rolling. In both of these processes, the geometry of the contact area with respect to the workpiece dimensions is the significant parameter. Thus, in shear forging, low feeds, small roller angles, and large nose radius or flat on the roller will tend to increase the circumferential dimension of the tube--hence an increase in its diameter. In internal shear forging, this same situation will result in the tube becoming tight against the die. It is obvious that if and when the workpiece has been preheated or if it develops high temperatures due to the mechanical work input, then, upon cooling, there will be additional changes in the diameter of the spun tube. This, of course, will be helpful in the subsequent removal of the part from the die.

An additional dimensional change that has been observed in external shear forging is bell mouthing.* In forward shear forging of tubes, the free end of the tube (i.e., the unspun end) has a tendency to expand circumferentially even though the section being reduced in thickness is still quite a distance away (Figures 10 and 19). One solution to this problem is to use a simple restraining ring on the free end of the tube.

* In internal shear forging, the free end was found to decrease in diameter, leading to nosing rather than bell mouthing.

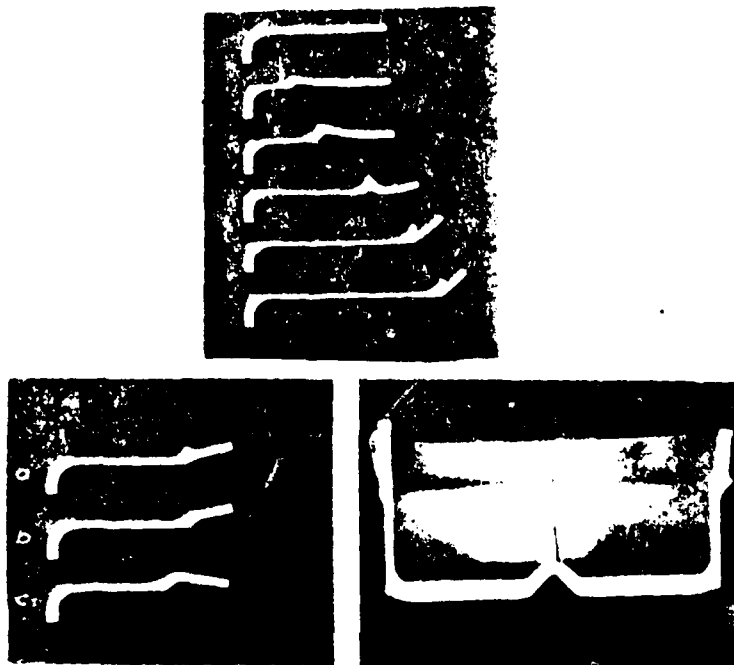


Figure 19. Buildup in various stages of shear forging (top) and influence of roller nose radius on buildup formation (bottom).²²

However, studies reported in the literature have identified the significant parameters that play a role in this phenomenon. This subject is closely related to the surface deformations that take place adjacent to the roller-workpiece contact zone.

These surface deformations have been studied systematically, as described in References 22, 27, 28, 31, and 32 with additional examples being given in References 24, 33, 38, and 39. Typical examples of buildup are shown in Figures 19 to 25.

It has been shown that the important parameters in these deformations are: reduction in wall thickness, roller angle (or its nose radius if round), the angle of tilt of the roller axis with respect to the mandrel axis, and feed. The surface deformation (also called buildup or

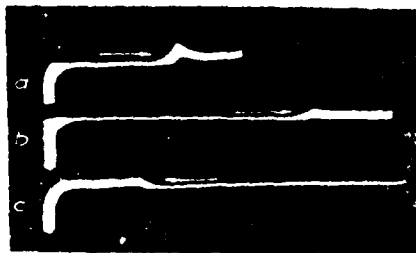


Figure 20. Stages in shear forging with three different methods using the same roller. (a) Roller axis parallel to mandrel axis, i.e., skew angle = 0° ; (b) inclined roller axis, skew angle = $+20^\circ$, direction of feed from cup base to cup flange; (c) inclined roller axis, skew angle = 20° , direction of feed from cup flange to cup base.²²

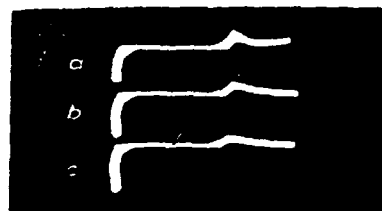


Figure 21. Influence of skew angle on buildup formation. (a) 0° , (b) 10° , (c) 20° .²²

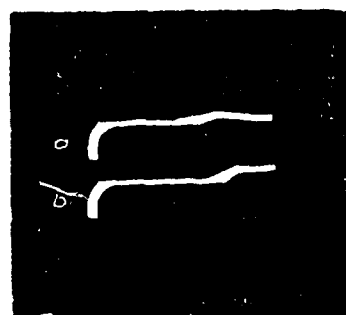


Figure 22. Influence of contact angle α of roller on buildup formation. (a) $\alpha = 10^\circ$, (b) $\alpha = 25^\circ$.²²

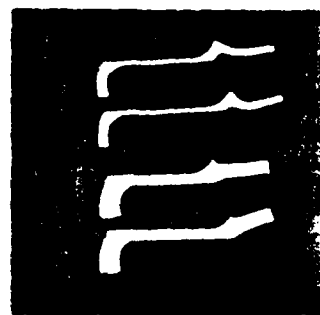


Figure 23. Influence of original wall thickness on buildup formation.²²

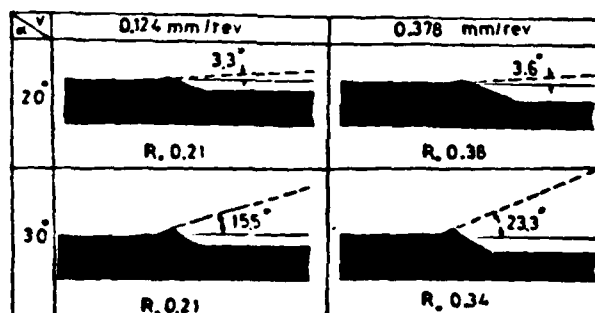
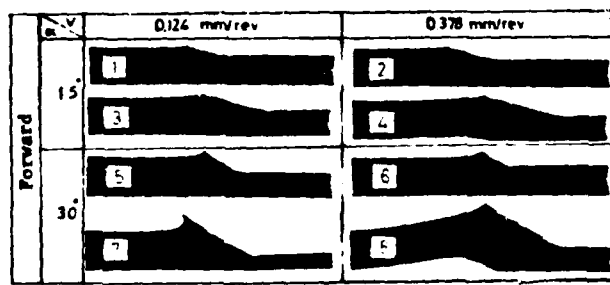


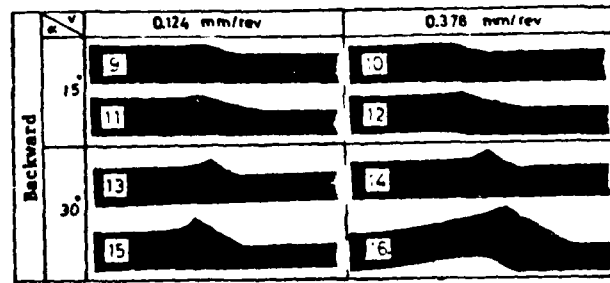
Figure 24. Comparison of calculated angles of buildup with actual buildup profiles in forward shear forging.³¹

wave) changes and becomes more prominent as shear forging progresses along a particular workpiece. It further appears that the ductility of the material also plays a role to the extent that soft, ductile materials have a greater tendency to form such buildup ahead of the roller.

As can be seen from the series of samples shown in Figures 19-25, such buildup increases with increasing reduction, roller angle, and feed. It decreases with increasing roller tilt angle and roller nose radius. It has been shown that there is no appreciable difference in buildup between forward and backward shear forging under otherwise similar processing conditions, as seen in Figure 25.



(a)



(b)

Figure 25. Influence of roller angle, feed rate, and reduction on buildup and distortion ahead of roller.³¹

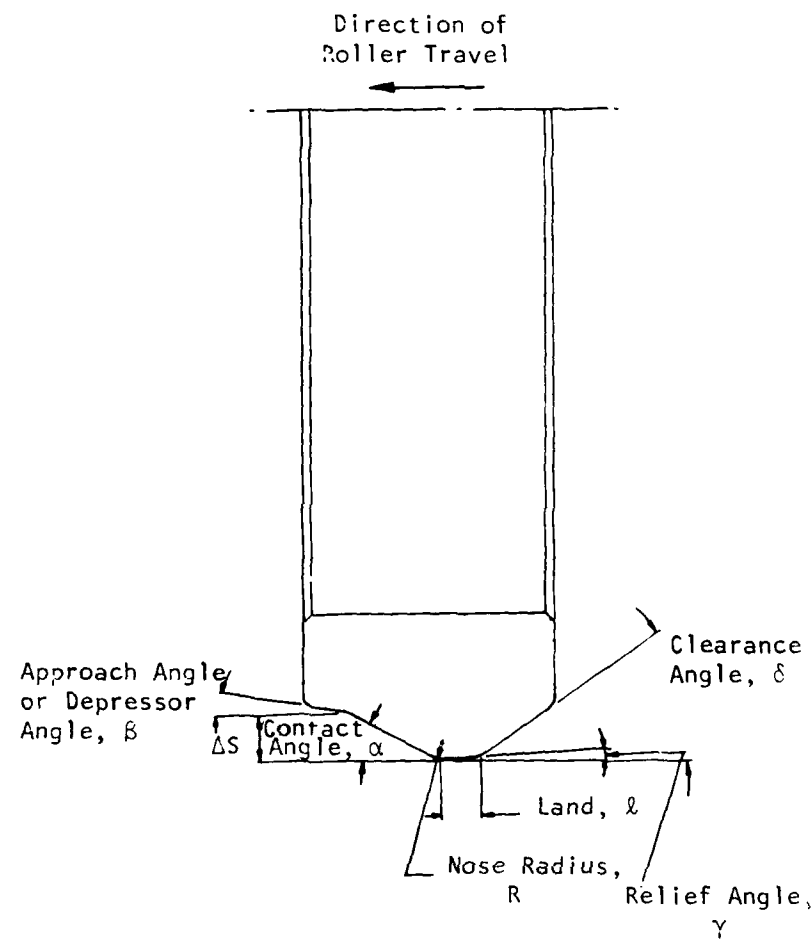


Figure 26. Roller geometry and nomenclature.

In addition to controlling the relevant parameters to reduce buildup, a practical method is to have a second flat roller whose cylindrical surface is tangent to the outer diameter of the unspun section of the tube. In this way, any tendency for buildup will be continually suppressed by the cylindrical roller. It is also possible to design the working roller to have an approach or depressor angle (i.e., flat land ahead of the contact angle) to serve the same purpose (Figure 26).

By such techniques, a buildup-free deformation zone can be generated, thus minimizing surface defects on the spun surfaces (Figure 27). The disadvantage in the second technique is that a new roller geometry is needed for each range of heights, as indicated by ΔS in Figure 26.



(a)



(b)

Figure 27. Section through workpiece showing material flow.
(a) *Using rollers without approach angle,*
(b) *using rollers with approach angle.³³*

3.3.3 Forces in Shear Forging of Tubes

Because of their relevance to the design of shear forging equipment and components, the three principal forces in this process have been studied both analytically and experimentally. The technical literature on this subject is given in References 21, 22, 24, 25, and 32-40. It appears that, in most studies, the experimental data obtained on forces have been plotted against process parameters and no effort has been made to obtain analytical or empirical formulas for forces. Furthermore, there appear to be no studies published on internal shear forging. (Most of the theoretical studies on forces have been in shear forging of conical workpieces, also known as shear spinning.)

It is not within the scope of this review to present a detailed theoretical analysis of forces in shear forging of tubes; rather, some results of previous attempts will be presented, with empirical relationships given for the benefit of design engineers.

a) External Shear Forging. There appear to be two studies in the literature pertaining to expressions for forces, References 22 and 40. In the former study, the following formulas are given for the forces in forward shear forging of tubes:

$$F_t = \sigma(\Delta t)f$$

$$F_a = \sigma(\Delta t) [rf \tan \alpha]^{\frac{1}{2}}$$

$$F_r = \sigma(\Delta t) [rf \cot \alpha]^{\frac{1}{2}}$$

where

σ = average flow stress workpiece

Δt = bite, i.e., $(t_0 - t_f)$, where t_0 = original thickness and t_f = final thickness

r = $(D_M D_R)/(D_M + D_R)$ where D_M and D_R denote the diameter of the mandrel and rollers, respectively

f = roller feed rate

α = roller angle.

Subscripts t, a, and r refer to tangential, axial, and radial, respectively.

In the second study,⁴⁰ the following formulas have been derived:

$$F_t = K_t \sigma' t_0 f$$

$$F_a = K_a \sigma' t_0 [D_R f \tan \alpha]^{\frac{1}{2}}$$

$$F_r = K_r \sigma' t_0 [D_R f \cot \alpha]^{\frac{1}{2}}$$

where K_t , K_a , and K_r are parameters to be obtained from Figure 26, and $\sigma' = 1.15 \sigma_0$, where σ_0 is the yield stress of the workpiece material.

Figure 28 also shows the results of the two methods of analysis that have been used--namely, strip solution and slipline solution. It also shows the results for backward shear forging of tubes.

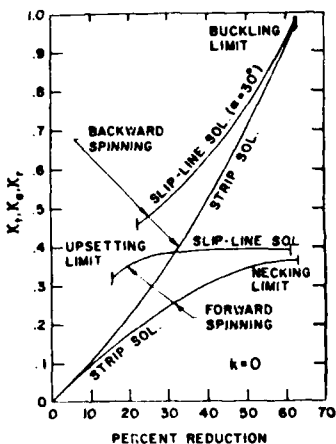


Figure 28. Force coefficients in forward and backward shear forging.⁴⁰

The two sets of formulas are essentially the same and are in approximate agreement with each other when reasonable values are substituted, using the strip solution for the second set of formulas.

The foregoing studies do not include the friction and redundant work during deformation. Furthermore, they are based on an ideal contact between the roller and workpiece (at an angle, α) but neglect the effects of the roller nose radius and relief angle. All of these neglected factors could play a significant role on the magnitude of forces.

In experimental studies, it has been shown⁴¹ that when shear forging aluminum, mild steel, and stainless steel, the actual tangential and radial forces are about twice those predicted by theory, whereas the axial force agrees well with theory for backward shear forging and is about 50% higher than the predicted values for forward shear forging.

As a guide for estimating actual forces, Figures 29 and 30 may be used for backward and forward shear forging of tubes, respectively. They are based on experimental data and should be used only as guides because the influence of many process and material parameters can be significant.

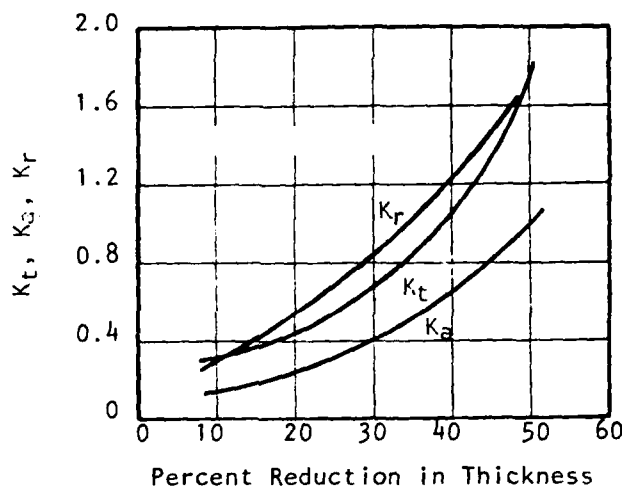


Figure 29. Force factors vs. thickness reduction in backward shear forging.⁴¹

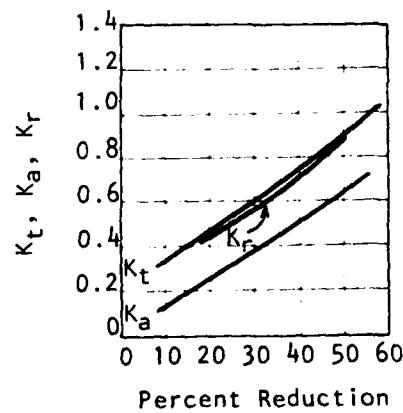


Figure 30. Force factors vs. thickness reduction in forward shear forging.⁴¹

b) Internal Shear Forging. As stated earlier in this review, there appear to be no studies reported on forces in internal shear forging of tubes in the literature. Because the deviation of forces have, in external shear forging as well as in many other metalworking processes, been largely based on the magnitude of the contact area between the tool and the workpiece, it is possible to obtain an approximate expression for internal shear forging forces.

The projected axial areas of contact between the roller and the tube for the two cases are shown in Figure 31. The bite is given by Δt , and the significant dimension is the length of the arc ab . Assuming that $\Delta t \ll D_R$ or D_M , it can be shown that the length ab is given by,

and

$$ab_{ext} \approx [D_R \Delta t / (1 + D_R/D_M)]^{1/2}$$

$$ab_{int} \approx [D_R \Delta t / (1 - D_R/D_M)]^{1/2}$$

If one further assumes that, for the same feed (f), bite (Δt), and roller angle (α), the contact area will be directly proportional to the length ab , then the ratio of forces for internal to external shear forging will be,

$$F_{int}/F_{ext} = [(1 + D_R/D_M) / (1 - D_R/D_M)]^{1/2}$$

For the present study where $D_R = 216$ mm or 8.5 in. and $D_M = 406$ mm or 16 in., this ratio will then be 1.8. Thus, the forces in internal shear forging would be nearly twice as much as for the external case under otherwise identical conditions.

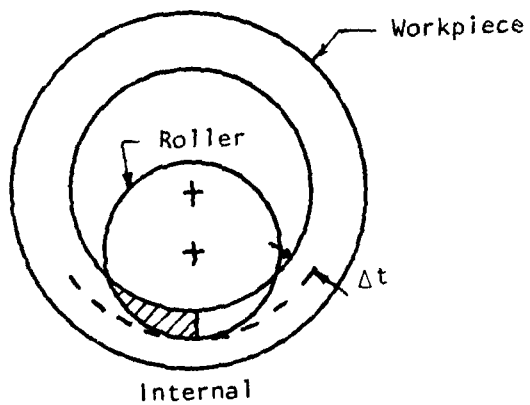
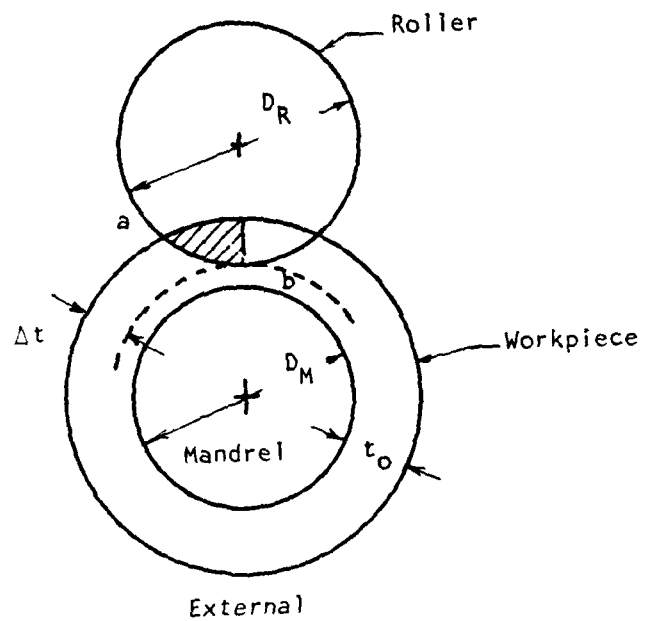


Figure 31. Contact geometry in external and internal shear forging of tubes.

4. 2014 ALUMINUM ROLLING EXPERIMENTS

The principal aim of this task (Task 1) of the Basic Effort was to study the deformation processing characteristics of aluminum alloy 2014, to establish the starting condition of the alloy, and to predict its response to deformation during internal shear forging.

4.1 TASK OBJECTIVES

In shear forging, the material is subjected to a reduction in thickness in an incremental fashion similar to the rolling process. Furthermore, because the current method of manufacture for these missile structures utilizes rolled stock, it was decided to study the rolling characteristics of this alloy and to establish, if possible, the desired processing parameters for internal shear forging. Both material-related variables and processing variables were considered in the exploratory study. The material-related variables included alloy temper; size and thickness of the work-piece; starting, intermediate, and final microstructures; and the presence and distribution of secondary phases. The process-related variables involved selection of parameters like reduction per pass, rolling temperature, lubricant, rolling speed, number of rolling passes, heat treatment between passes, and post-rolling heat treatment. In selecting the range of these variables, due consideration was given to the interrelationships between temperature, reduction, and strain rate as these variables directly influence the reduction behavior and final properties of the rolled material. Initial roll temperature, temperature and thickness of the starting work-piece, and the heat generated during plastic deformation also influence the final properties and microstructure of the rolled product.

The alloy 2014 is a heat-treatable age-hardening alloy and contains Al with Cu, Mg, and Si as the main alloying elements. Addition of Si enhances the response to artificial aging (T6 temper), with the final strength being higher than for the naturally aged (T4) condition. This

alloy is widely used in structural applications. For deformation processing, it is desirable that the alloy be in a fully annealed (0-temper) condition. The fully annealed temper yields stabilized precipitate phases in a matrix which has high ductility and can undergo a considerable amount of plastic deformation.

For the present experiment, the 2014 alloy could not be procured in the fully annealed condition. Therefore, a 1-inch thick rolled plate was procured in the T651 temper (solution treated, stretched 0.5-3%, and then artificially aged). A 150 x 150 x 25 mm (6 x 6 x 1 in.) plate of the 2014-T651 plate was then annealed at 413°C (775°F) for 2 hours to achieve the annealed condition (0-temper) before processing.

Microstructures were examined by optical microscopy as well as scanning electrom microscopy (SEM). Energy-dispersive X-ray (EDX) analysis was employed for all identification of various constituent phases. All microscopy specimens were etched with Keller's reagent. Tensile strength values quoted here were obtained from the longitudinal (parallel to rolling) direction unless specified otherwise.

4.2 STARTING MATERIAL

Table 1 gives the tensile properties and chemical composition of the 2014-T651 alloy in the as-received condition. The as-received microstructure displayed elongated recrystallized grains interspersed with particles of precipitate phases. SEM examination at higher magnification (1500X) revealed the presence of two kinds of precipitate phases, CuAl₂ (Figure 32a) and (FeMn)₃SiAl₁₂ (Figure 32b). Spot EDX analysis confirmed the presence of the above phases.

The mechanical properties of the 2014-0 alloy (after annealing for two hours at 413°C from T651 condition) are given in Table 2. The indicated value of 192 MPa UTS is close to the specified value (202 MPa) for

TABLE 1. MECHANICAL PROPERTIES AND CHEMICAL COMPOSITION OF AS-RECEIVED 2014-T651 ALUMINUM ALLOY ROLLED PLATE

Item	Measured	Specification
<u>Mechanical Properties</u>		
UTS	295 MPa (42.9 ksi)	483 MPa (70.0 ksi)
Elongation	6% (in 25 mm)	13% (in 50 mm)
<u>Chemical Composition (wt%)</u>		
Chromium	0.01	0.10 max
Copper	4.46	3.90-5.00
Iron	0.52	1.00 max
Magnesium	0.52	0.20-0.80
Manganese	0.72	0.40-1.20
Silicon	0.91	0.50-1.20
Titanium	0.02	0.15 max
Zinc	0.18	0.25 max

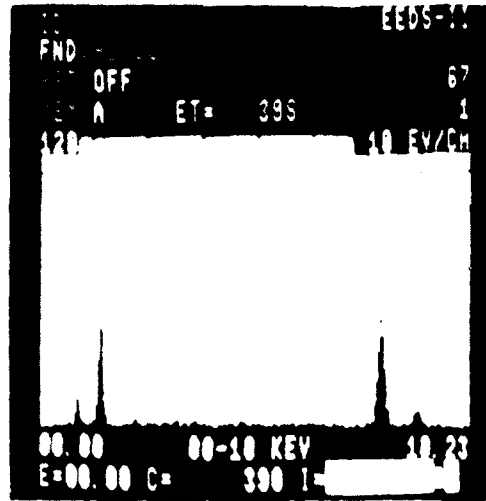
TABLE 2. MECHANICAL PROPERTIES OF 2014-O ALUMINUM ALLOY PLATE USED AS STARTING MATERIAL IN ROLLING EXPERIMENTS (Annealed at 413°C-2 hr)

Item	Longitudinal	Transverse
Yield strength (0.2% offset)	118 MPa (17.1 ksi)	94 MPa (13.6 ksi)
UTS	192 MPa (27.9 ksi)	202 MPa (29.3 ksi)
Elongation (in 25 mm gage length)	14%	20%
Reduction in area	43.9%	34.6%



SEM No. 4115

1500X

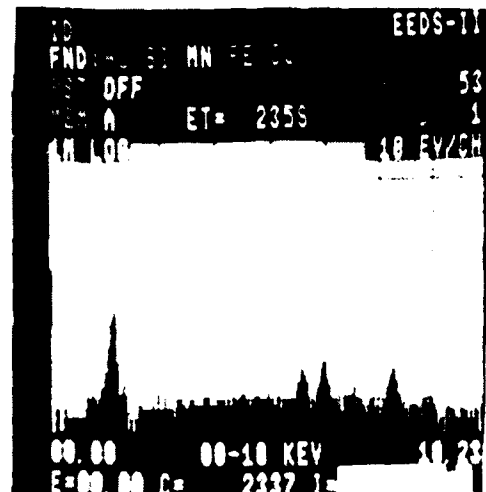


(a)



SEM No. 4111

1500X



(b)

Figure 32. Precipitate phases in 2014-T651 as-received plate.
(a) CuAl_2 , (b) $(\text{FeMn})_3\text{SiAl}_{12}$.

the 2014-0 condition. Detailed microstructural examination by SEM and EDX revealed that the cooling after annealing treatment was probably not slow enough, because in addition to remnants of CuAl₂ and (FeMn)₃SiAl₁₂ phases, a very finely dispersed phase was also detected in the matrix. Figure 33 shows a high-magnification (5000X) view of this phase. It was identified to be a precursor of the CuAl₂ phase. Since this phase precipitated at a lower temperature, its presence should not interfere with deformation processing at higher temperatures (150-300°C) where it would go back into solid solution.

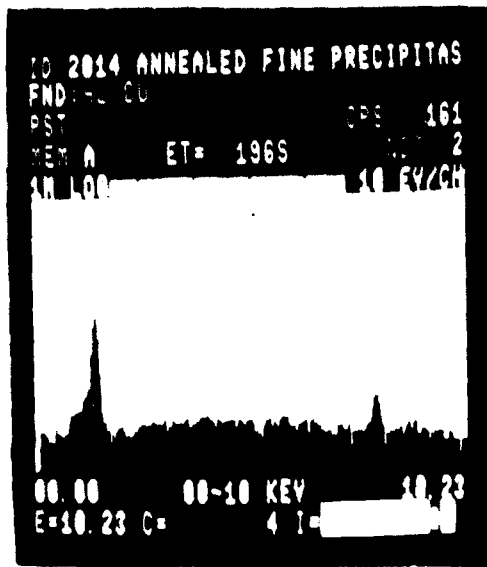


Figure 33. Finely dispersed precipitate phase observed after annealing (prior to rolling).

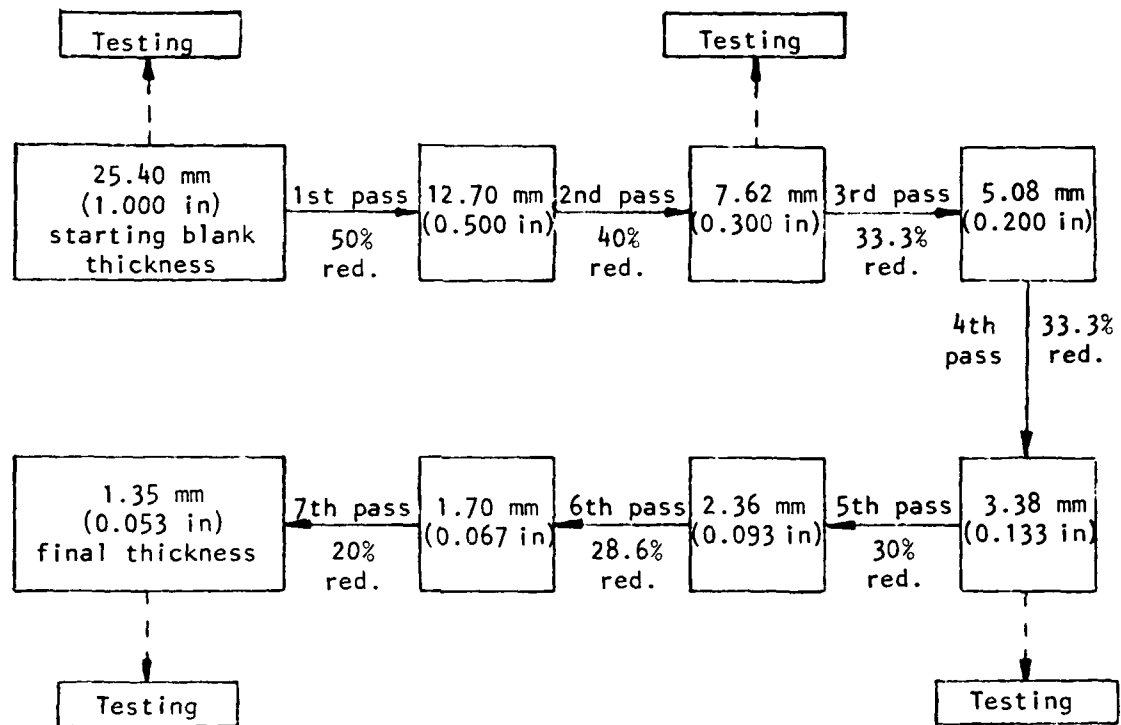
4.3 ROLLING EXPERIMENTS

For all rolling experiments, the workpiece was 150 x 150 x 25 mm in dimensions and was in the annealed condition. Each experiment involved seven passes in accordance with the rolling schedule given in Figure 34. A Fenn type 122 rolling mill was used for the present study. The starting roll temperature was 66°C (150°F) in all cases. Figure 35 presents a summary of all the rolling experiments which were carried out in the present study. Details of the various parameters used in these experiments and post-rolling heat treatments to obtain T4 and T6 tempers are also given in Figure 35.

As indicated in Figure 35, samples for mechanical testing were taken after the second, fourth, and seventh passes for the 149°C (300°F) and 316°C (600°F) rolling experiments. Some of these samples were mounted, polished, and etched for metallographic examination to study the micro-structural characteristics of the rolled specimens. Highlights of the rolling experiments are presented below.

Table 3 summarizes the details of the 149°C (300°F) rolling experiment which was carried out to evaluate the performance of various lubricants. Performance of all three lubricants was similar in terms of the as-rolled surface finish. However, the Aquadag lubricant was found to be marginally better than the others in minimizing the roll-separating force as determined by thickness reduction allowing for roll deflection. Therefore, Aquadag was used in subsequent rolling experiments.

In order to test the effect of rolling speed, a rolling experiment was carried out at 149°C (300°F) with Aquadag lubricant. At rolling speeds of 0.4, 1.2, 2.5, and 4.2 m/s (75, 245, 490, and 817 fpm), a thickness reduction of 95% was obtained after nine passes in each case. These rolled specimens were mechanically tested in the as-rolled condition and also after T4 and T6 aging treatments (Figure 35). Table 4 gives the results of these experiments. As expected, T6 specimens show higher UTS for all speeds. Over the range of rolling speeds studied, the rate of deformation, (i.e., rolling speed) seemed to have no significant influence on the mechanical properties.



1. The above numbers indicate planned reductions only; actual values differ slightly.
2. Percentage reduction decreases progressively in accordance with schedule for internal shear forging, which requires the percentage reduction to be roughly proportional to the blank thickness.

Figure 34. Reduction sequence for rolling of 2014-0 aluminum alloy.

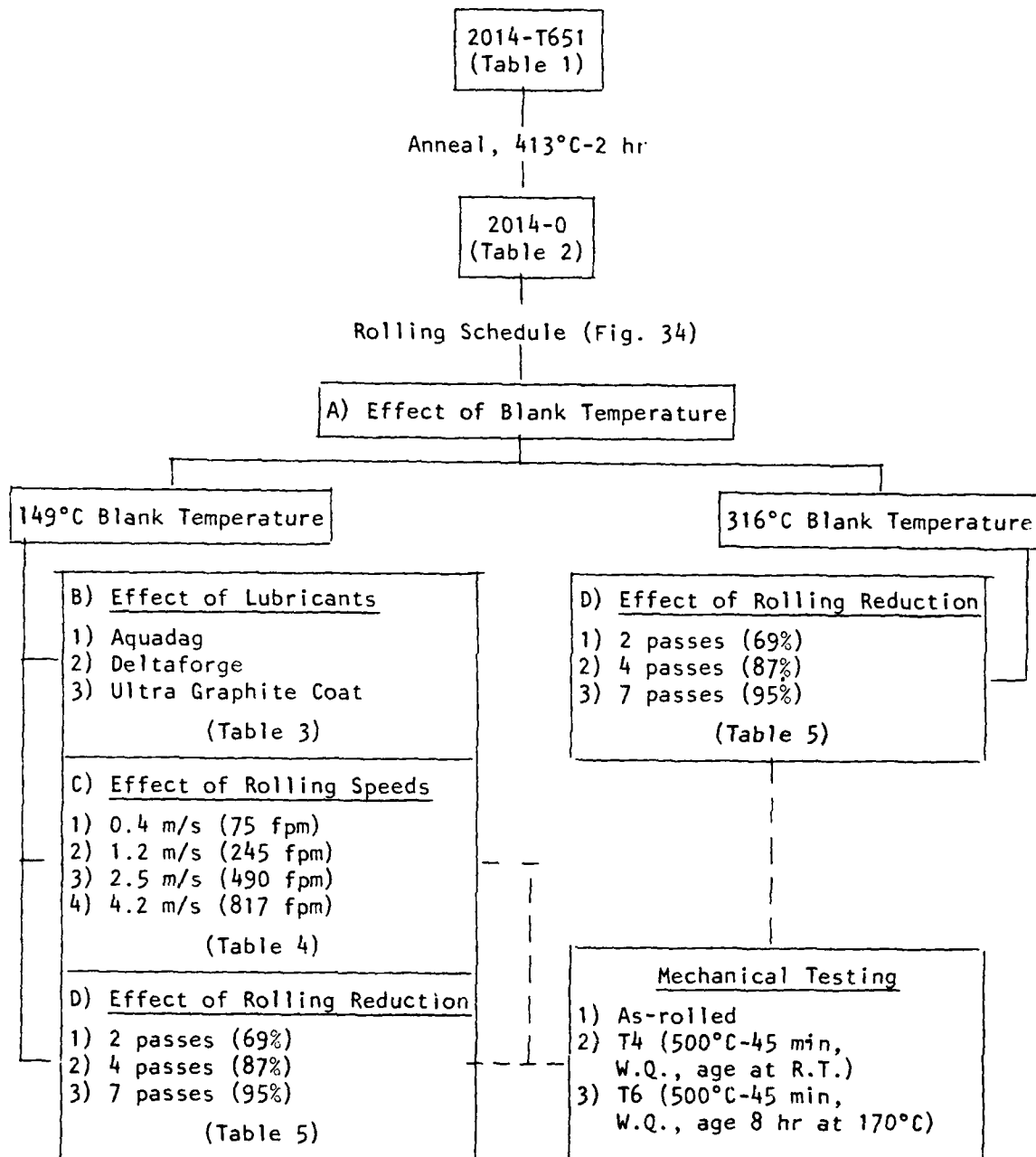


Figure 35. Summary of rolling experiments for 2014 aluminum alloy.

TABLE 3. ROLLING EXPERIMENTS WITH 2014-0 ALUMINUM ALLOY WITH DIFFERENT LUBRICANTS

Pass No.	Planned Reduction, %	Planned Thickness, mm (in.)	Roll Gap mm (in.)	Actual Thickness Obtained With Given Lubricant, mm (in.)		Actual Reduction With Given Lubricant, %	Ultra Graphite Coat	Delta-forge Aquadag	Delta-forge Aquadag	Graphite Coat
				Ultra	Graphite Coat					
1	50	12.70 (0.500)	11.35 (0.447)	13.46 (0.530)	13.69 (0.539)	13.77 (0.542)	47	46	46	46
2	40	7.62 (0.300)	6.35 (0.250)	8.03 (0.316)	8.28 (0.326)	8.48 (0.334)	40	36	36	38
3	33	5.08 (0.200)	3.76 (0.148)	5.23 (0.206)	5.26 (0.207)	5.56 (0.219)	35	36	36	34
4	33	3.38 (0.133)	2.06 (0.081)	3.25 (0.128)	3.38 (0.133)	3.71 (0.146)	38	36	36	34
5	33	2.36 (0.093)	1.04 (0.041)	2.21 (0.087)	2.39 (0.094)	2.51 (0.099)	32	31	31	32
6	28	1.70 (0.067)	0.36 (0.014)	1.45 (0.057)	1.63 (0.064)	1.73 (0.068)	34	32	32	31
7	20	1.35 (0.053)	0.25 (0.010)	1.30 (0.051)	1.37 (0.054)	1.42 (0.056)	11	16	16	18

Fenn type 122 rolling mill; speed 0.4 m/s (75 fpm); roll temperature 66°C (150°F); blank temperature 149°C (300°F).

TABLE 4. EFFECT OF ROLLING SPEED AND HEAT TREATMENT
ON MECHANICAL PROPERTIES OF ALUMINUM ALLOY 2014

Testing Condition	UTS, MPa (ksi)				Elongation in 25 mm, %			
	0.4 m/s	1.2 m/s	2.5 m/s	4.2 m/s	0.4 m/s	1.2 m/s	2.5 m/s	4.2 m/s
As-rolled	405 (58.7)	323 (46.8)	328 (47.5)	369 (53.5)	3.6	7.6	6.0	5.6
T4	356 (51.6)	403 (58.4)	335 (48.6)	339 (49.1)	11.8	12.4	14.0	9.6
T6	396 (57.4)	458 (66.4)	483 (70.0)	379 (55.0)	10.4	14.8	5.6	11.6

Notes:

1. Aquadag was used as lubricant.
2. 95% total rolling reduction (in 9 passes).
3. 149°C (300°F) blank temperature at start of each pass.
4. 66°C (150°F) roll temperature.
5. Test direction was longitudinal, i.e., parallel to rolling direction.
6. Tensile specimens were 6.4 mm (0.25 in.) width x as-rolled thickness x (1.00 in.) gage length.

Based on the results presented above, Aquadag lubricant and a rolling speed of 0.4 m/s (75 fpm) were selected for rolling experiments at 149°C (300°F) and 316°C (600°F). Figure 35 gives the experimental details of these two rolling experiments, and Table 5 lists the mechanical properties obtained after rolling at various degrees of reduction and post-rolling heat treatment. Table 5 shows that the as-rolled strength increases with increasing percent reduction at both temperatures. As-rolled specimens at 149°C exhibit poor ductility, with the elongation decreasing with increasing reduction. This may be due to an additional strain-hardening effect because of the presence of a fine precipitate phase in the 2014-0 condition (Figure 33). Reversion of this phase was probably incomplete at 149°C. Slightly higher UTS values were achieved for 95% reduction in

nine passes at 149°C as shown earlier in Table 4. After 316°C rolling, specimens display fairly high ductility. Both for 149°C and 316°C specimens, solution heat treatment followed by T4 and T6 aging achieved higher strengths, although the values quoted in Table 5 are slightly lower than those specified in the literature (UTS: for T4 = 427 MPa or 62 ksi, for T6 = 483 MPa or 70 ksi).

TABLE 5. EFFECT OF BLANK TEMPERATURE AND ROLLING REDUCTION ON MECHANICAL PROPERTIES OF ALUMINUM ALLOY 2014

Passes	Total Reduction in Thickness, %	Testing Condition	UTS, MPa (ksi)		Elongation in 25 mm, %	
			149°C ^a	316°C ^a	149°C ^a	316°C ^a
0	0	Annealed	192 (27.9)	192 (27.9)	14.0	14.0
2	69	As-rolled	229 (33.2)	219 (31.8)	11.7	16.3
		T4	328 (47.6)	325 (47.1)	22.2	18.7
		T6	372 (53.9)	377 (54.7)	21.8	22.9
4	87	As-rolled	254 (36.9)	332 (48.1)	9.7	13.6
		T4	321 (46.5)	345 (50.0)	18.6	18.6
		T6	487 (70.6)	392 (56.9)	21.5	20.2
7	95	As-rolled	280 (40.6)	396 (57.4)	3.7	17.9
		T4	325 (47.1)	318 (46.1)	12.0	14.0
		T6	362 (52.5)	373 (54.1)	--	15.1

Notes:

Roll temperature: 66°C (150°F)

Rolling speed: 0.4 m/s (75 fpm)

Test direction: longitudinal (L)

Specimen geometry: 6.4 mm (0.25 in.) width x as-rolled thickness x 25.4 mm (1.00 in.) gage length

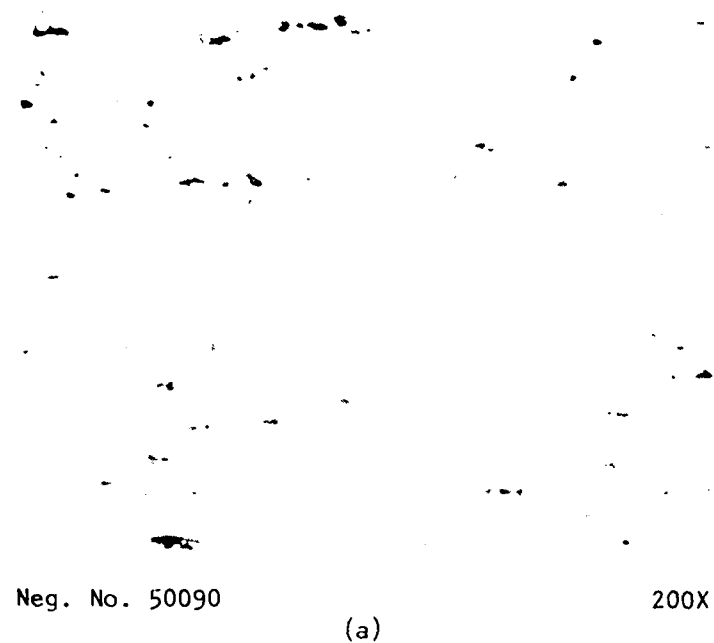
^aBlank temperature at commencement of each pass.

The mechanical properties achieved in heat-treatable alloys are determined by microstructural changes which accompany processing and heat treatment. A study of microstructures is therefore essential at various stages of the processing sequence. The following section summarizes microstructural observations made during the course of the present experiments.

4.4 MICROSTRUCTURAL OBSERVATIONS

Macroscopic samples of annealed and rolled specimens were taken from the longitudinal, long-transverse, and short-transverse directions and were examined, after etching, at a low magnification (25X) for visible flaws like cracks, folds, and inclusions. Metallographic specimens were prepared from 149°C and 316°C rolled specimens from all three rolling directions after 69, 87, and 95% reductions. These specimens were examined by optical microscopy (100 to 250X) and SEM (up to 1500X) to reveal the grain structure, material flow, grain fragmentation, and fragmentation and redistribution of the precipitate phases CuAl_2 and $(\text{FeMn})_3\text{SiAl}_{12}$ which were present in the 2014-0 condition. EDX analysis was used on SEM specimens to identify various phases.

Specimens rolled at 149°C displayed elongated and fragmented grains. The grains were elongated in the direction of working and flattened in the thickness direction. No pronounced difference was noted in grain structures after various reduction levels. This may be due to the intermediate annealing that was used between passes to restore the temperature of the workpiece to 149°C. Figure 36a shows the as-rolled structure, in the long-transverse direction, after 95% reduction at 149°C. With increasing reduction, the banded precipitate structure became more random, the precipitate size grew slightly; however, no visible difference was detected in precipitate density. Both CuAl_2 (with some Mg) and $(\text{FeMn})_3\text{SiAl}_{12}$ precipitates were present. Figure 36b shows an SEM micrograph at 500X for the same specimen. White precipitates are the CuAl_2 phase, and the gray angular precipitates belong to the $(\text{FeMn})_3\text{SiAl}_{12}$ phase.



Neg. No. 50090

200X

(a)



SEM No. 4131

500X

(b)

Figure 36. Photomicrographs, (a) optical and (b) SEM, of as-rolled structure after 95 percent reduction by rolling at 149°C.

For 316°C rolling experiments, the grain structure tended to coarsen slightly with increasing reduction. Since 316°C is probably in the recrystallization regime for this alloy, and rolled specimens were reheated to 316°C between passes, some recrystallization and grain size changes are expected to occur. Figure 37a shows a typical long-transverse section showing precipitate and grain structures after 95% reduction at 316°C. EDX analysis on SEM specimens showed the presence of only the CuAl₂ phase. A very fine precipitate was found to develop after 316°C rolling, and it could be detected only at higher magnifications (Figure 37b). As mentioned before, a similar phase was also detected after annealing. This phase probably disappears at the 316°C rolling temperature, but reappears upon cooling from the rolling temperature.

The main purpose for conducting post-rolling heat treatment to obtain T4 and T6 conditions was to check whether the final rolled product could be obtained in these high-strength tempers irrespective of the rolling temperature and percent reduction. The solution treatment for all specimens was 500°C (930°F), and the time at temperature was 45 min. After solution treatment, specimens were water-quenched and then aged at room temperature to obtain the T4 temper. For the T6 temper, quenched specimens were artificially aged at 170°C (340°F) for 8 hr.

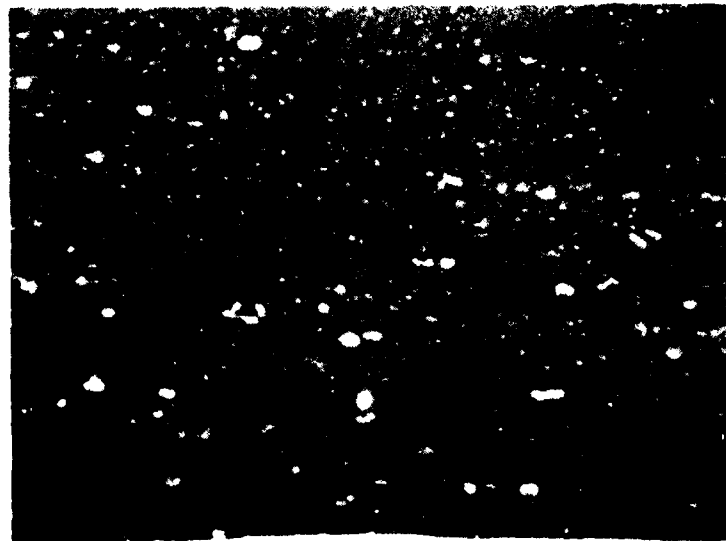
Microstructural examination of solution treated and aged specimens from the 149°C experiment revealed that the actual solution treatment temperature was probably higher than 500°C. This resulted in melting of the eutectic and solid solution constituents at grain boundaries. Consequently, upon subsequent aging to T4 and T6 tempers, this brittle grain boundary phase persisted. Figure 38a shows the worst case of this grain boundary melting phenomenon in the case of 95% reduction followed by solution treatment and natural aging to achieve T4 temper. By contrast, solution treated and aged specimens from 316°C rolling showed normal recrystallized grains with strengthening phases that were precipitated



Neg. 49879

200X

(a)



SEM No. 4120

500X

(b)

Figure 37. Photomicrographs, (a) optical and (b) SEM, of as-rolled structure after 95 percent reduction by rolling at 316°C.

Neg. 50136

(a)

100X

Neg. 49959

(b)

100X

Figure 38. Optical photomicrographs of samples rolled to 95 percent reduction, solution treated and naturally aged to the T4 condition. (a) 149°C rolling temperature (evidence of grain boundary melting during solution annealing); (b) 316°C rolling temperature (equiaxed recrystallized grains after T4 treatment).

during aging to achieve T4 and T6 tempers. An example of such a micro-structure is shown in Figure 38b for the case of 316°C rolling with 95% reduction and in the T4 condition. Figure 38b shows a long-transverse section. The presence of equiaxed recrystallized grains is to be noted.

4.5 CONCLUSIONS

The rolling experiments described above lead to the following important conclusions:

- 1) It is essential that the starting condition of the 2014 alloy for bulk deformation processing be in a completely annealed condition in order to achieve maximum ductility of the matrix with stabilized precipitates. In the present study, this condition was not achieved to the desired extent, perhaps because of the T651 temper of the starting material.
- 2) The present experiments indicate at higher temperatures, deformation rates (by changing the rolling speed) do not produce a pronounced change in the appearance of the grain structure. Shear forging of the proposed part may involve localized differences in deformation rates, but the present results indicate that this should not pose any serious problem.
- 3) Post-rolling heat treatment experiments demonstrate that the utmost care must be exercised during solution treatment in order to achieve the desired strength and ductility in the final product. Grain boundary melting can be avoided if the solution treatment is preceded by a homogenizing anneal at a lower temperature. Precise temperature control is, however, extremely important.

5. TOOLING DESIGN AND FABRICATION

5.1 SHEAR FORGING MACHINE

A heavy-duty engine lathe (LeBlond Model 2516) was converted into an experimental shear forging machine using the tooling described later in this section. The lathe specifications are as follows:

• swing over bed and carriage wings	635 mm (25 in.)
• face plate diameter	597 mm (23½ in.)
• available number of spindle speeds	36
• feed range	0.114-6.604 mm/rev (0.0045-0.2600 in/rev)
• spindle speed range	10-1300 rpm
• maximum horsepower	40

5.2 BASIC CONSIDERATIONS IN TOOLING DESIGN

Some of the important aspects of tooling design for internal shear forging, based on the metalworking requirements imposed on the tooling components, are discussed below.

5.2.1 Die Construction

The high radial force in internal shear forging, particularly when a roller of small contact angle is used, causes diametral expansion of the shear forged part inside the die. While this problem could be alleviated somewhat by using a roller of adequate contact angle, it is doubtful that it can be avoided altogether. It was necessary, therefore, to design the die as a split construction that could be separated to enable part removal and yet retain sufficient strength and rigidity to withstand the forces generated during shear forging.

It is important to have a smooth surface on the inside of the die to allow unrestricted axial movement of the shear forged tube during the forming process and to attain a high degree of surface finish on the outside of

the part. Further, the inside of the die must possess adequate hardness (HRC 55-60) to withstand the localized contact/indentation type of loading imparted by the roller in internal shear forging.

5.2.2 Roller Design for Shear Forging

The nomenclature used for the rollers was illustrated earlier in Figure 26. The "nose radius" R is usually equal to the thickness of the spun part for most workpiece materials, but may be increased as the softness of the material increases.

The "contact angle" or "deformation angle" α is responsible for the relative magnitudes of the radial and axial components of force during shear forging and thus influences the selection of the size of roller bearings. Smaller values of α lead to higher radial components of force, increasing the tightness between the shear forged part and the external die. Too large a value of α could prove detrimental to surface finish and smooth flow of the material under the roller.

The "approach angle" or "depressor angle" β prevents the workpiece material from rising ahead of the roller in backward shear forging. The axial "extrusion" force, which causes the material to bulge out, increases with increasing α . Therefore, proper selection of the angle β will permit a greater angle α , resulting in a more efficient operation.

The "relief angle" γ and the "land" ℓ are largely responsible for the surface appearance on the inside of the internally shear forged part. Small values of γ and/or large ℓ values cause a burnishing effect, resulting in a bright surface finish. However, these may also increase the pressure between the tube and the die and cause local buckling in the walls of the tube.

The "clearance angle" δ is provided in order to keep the length of land small and, at the same time, to have enough material of roller behind the deformation zone to withstand the shear forging forces.

The value ΔS determines the maximum possible reduction in thickness per pass. The actual reduction in thickness ($t_0 - t_f$) should be just marginally smaller than ΔS in order to utilize the angle β effectively (Figure 26).

5.2.3 Design Parameters Affecting Surface Finish

The following factors have been shown to influence the overall surface finish of the end product:

- a) contact angle, α
- b) nose radius, R
- c) relief angle, γ
- d) surface finish of roller
- e) feed rate
- f) speed of shear forging.

These factors are discussed below.

a) Contact angle, α . A roller with a very small contact angle will cause high radial forces to develop that tend to expand the tube radially. Being prevented from doing so by the presence of the rigid external die, the shear forged tube could buckle circumferentially in the thin-walled region, particularly during the final pass, and cause a wrinkled surface on the final part.

Too large a value for α would increase the severity of distortion ahead of the roller in the deformation zone and could damage the inside surface of the tube.

Contact angles of about 30° have been found to result in good performance during shear forging.

b) Nose radius, R . It has been found that leaving the nose as a sharp corner causes a rough finish on the end product. On the other extreme, very large values of R tend to reduce the effective contact angle, increasing radial forces and the likelihood of circumferential wrinkling. As a rule of thumb, nose radii are selected to be equal to the thickness of the tube (after shear forging) for most materials, with sharper radii for stronger materials and somewhat larger radii for softer materials.

c) Relief angle, γ . This angle influences the inside surface finish of the shear forged part more than any other roller parameter. The surface left behind by the roller is a replica not of the leading edge but rather the trailing edge of the roller. There is a small amount of elastic recovery of the tube after deformation, and a small relief angle of $1-2^\circ$ allows this recovery to take place in contact with the trailing edge. A value of $\gamma = 0^\circ$ implies that this recovery will take place after the material passes the trailing edge with no contact with the roller itself. The same is true if γ is larger than 2° , and in such cases the surface of the tube is poor. A γ value of 1.5° would be near optimum, and this value was used in designing the shear forging roller.

By similar reasoning, the length of land ℓ should be about $3/16$ in. for optimum results. The length of the approach zone and the magnitude of the approach angle β depend on the tendency of the material to build up ahead of the roller, and they, too, govern surface finish. Optimum choice of these variables depends on the values of α and R .

d) Roller surface finish. A fine microfinish on the trailing edge of the roller is necessary in order to have smooth surface finish on the inside of the tube. While an ordinary grinding operation may prove adequate for the rest of the roller, the length of land on the trailing edge requires additional polishing with diamond paste to provide the necessary degree of finish ($2-3 \mu\text{in. rms}$).

e) Feed rate. The role of feed rate on surface finish is more predominant in the case of shear spinning of cones where the roller consists of a true radius throughout the deformation zone. For shear forging rollers of the type shown in Figure 26, higher feeds would not result in wavier surfaces. Even at high feeds, these rollers should provide satisfactory finish, all other parameters being satisfactory.

f) Speed of shear forging. The volume rate of deformation (dV/dt , in^3/min) can be expressed in terms of the die ID (D_M , in.), the original thickness of the tube (t_0 , in.), the feed rate (f , in/rev), and the spindle rpm (N) as:

$$\frac{dV}{dt} = \pi D_M t_0 f N$$

The product fN is the axial velocity V_A of the roller. For the same feed rate, a higher rpm means a greater rate of deformation of the material. The upper bound N for the process is governed by the horsepower available and the maximum permissible temperature rise of the workpiece.

5.3 INITIAL TOOLING DESIGN AND TRIALS

The tooling designed initially for shear forging the subshells is shown schematically in Figure 39. The die is chucked to the lathe spindle, and the overhang is supported by the steady rest. The workpiece, in the form of a 2014-0 aluminum ring, is located inside the die, rotated in conjunction with the die, and deformed by the axial traversal of the shear forging roller.

Assembly procedures were established to result in accurate alignment of the rotating parts with the axis of the lathe. The experimental setup is shown in Figure 40. Initial trials were restricted to observations of the principal motions involved in shear forging, i.e., the die rotation, roller rotation, roller axial feed, and roller radial feed.

The shear forging roller is shown assembled to the roller arm in Figure 41. The fine surface finish on the outside of the roller is to be noted. Figure 42 shows a side view of the die holder (extreme left), the die (the five peripheral holes are for shoulder screws holding the two halves of the die together), the steady rest (center) which supports the die, and the shear forging roller (extreme right).

During operation (Figure 43), the aluminum alloy workpiece (1) is first preheated to the forming temperature by an oxyacetylene torch (2) and is then internally shear forged by the axial movement of the shear forging roller (3) at a preset reduction (allowing for deflection). The load is transmitted through the workpiece to the rotating external die (4), whose deflection is restrained by a three-roller steady rest (5). The oxyacetylene torch is kept on during the operation to maintain the forming temperature during roller traversal.

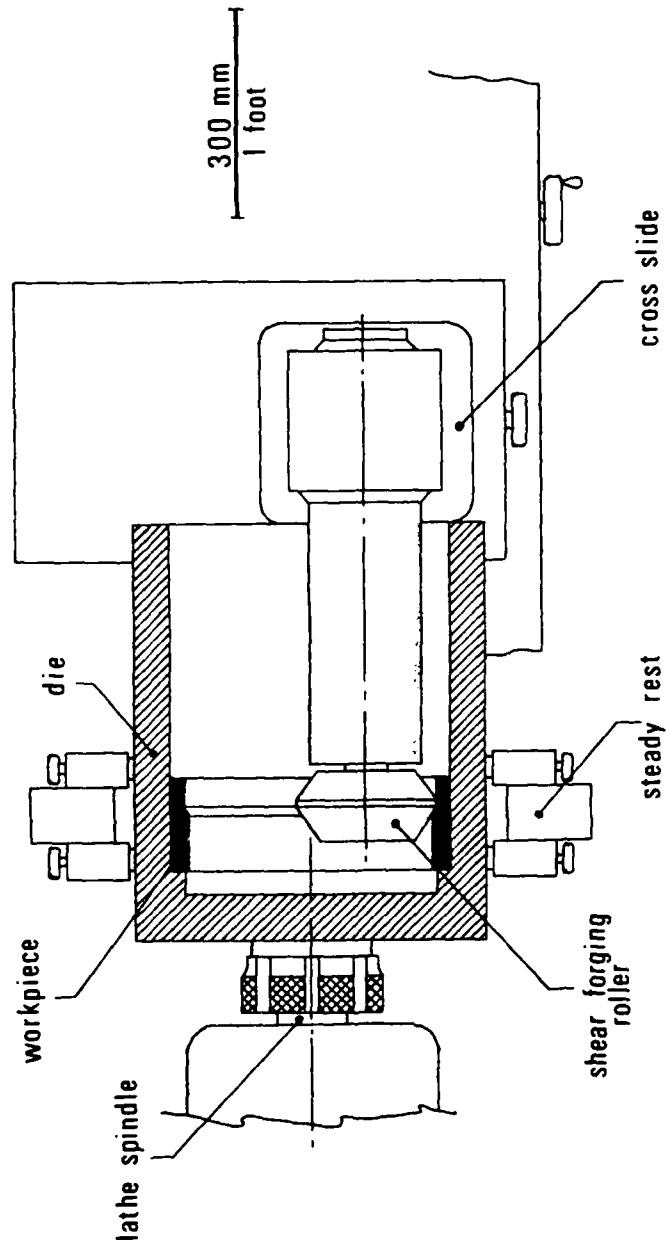


Figure 39. Initial tooling design for internal shear forging.



Neg. No. 51375

Figure 40. Experimental setup for internal
shear forging.



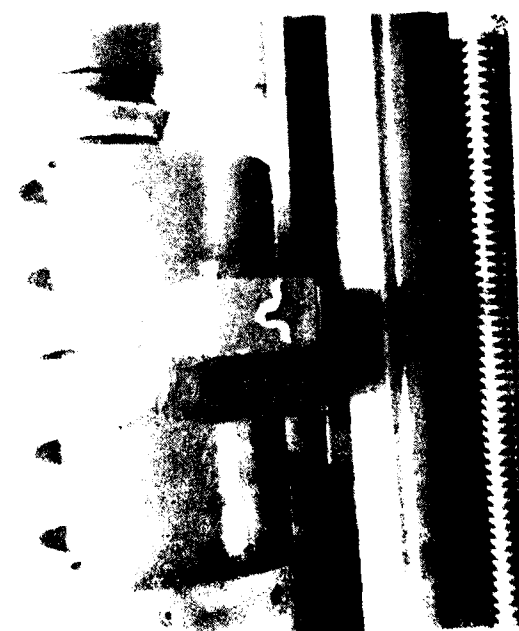
Neg. No. 51372

Figure 41. Shear forging roller unit.



Neg. No. 51839

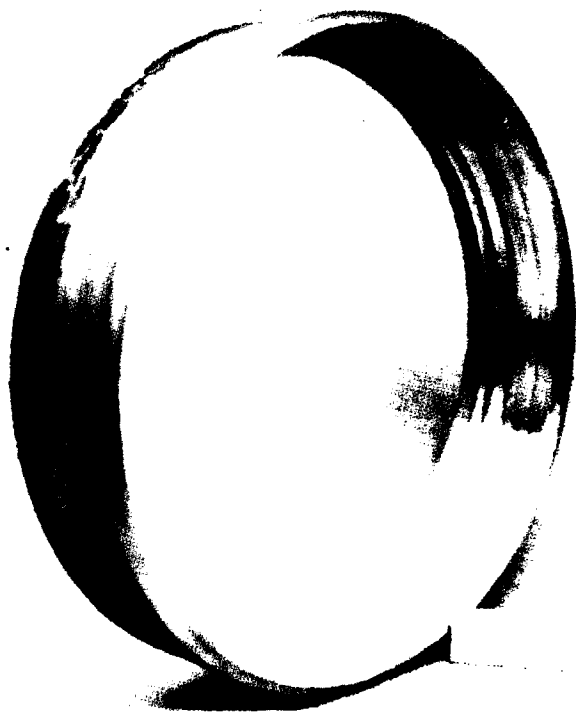
Figure 41. Initial tooling setup for internal shear forging. Aluminum alloy workpiece (1) is heated by an oxyacetylene torch (2) and deformed by the shear forging roller (3) against the die (4). Arrow indicates groove formation on die from high-pressure contact with steady rest rollers (5).



Neg. No. 51371

Figure 42. Side view of tooling for internal shear forging.

It was seen during the initial trials that adequate shear forging reductions could not be taken on account of excessive deflection of the tooling away from the preset reduction. Further, even when this deflection could be contained, the steady-rest rollers indented the die quite deeply (see arrow in Figure 43), preventing significant reductions from being taken. The maximum deformation that was permitted by the original tooling is seen in Figure 44.



Neg. No. 51841

Figure 44. 2014 aluminum alloy ring, partially deformed by internal shear forging. The experiment was interrupted due to excessive deflection and die indentation by steady rest rollers.

5.4 TOOLING MODIFICATIONS

To minimize deflections and enable the lathe to perform capably under the high forces generated during shear forging, the loading and support members of the tooling were "boot-strapped" together (Figure 45). The loading path thus generated would go from the roller arm directly to the interconnected support arm, with load transfer to the lathe possible only in the event of gross misalignment.

The modified tooling assembled in IITRI's LeBlond 2516 engine lathe is shown in Figure 46. The principal components are the die (A); a support roller (B) mounted on the support roller arm (C); a shear forging roller (D) mounted on the shear forging roller arm (E) which pivots with respect to the support roller arm about the swivel pin (F). Wall thickness reductions can be set by tightening or loosening the adjustment screw (G) at the aft end of the roller assembly. A set of oxyacetylene torches (H) provides workpiece heating during shear forging, while the carriage arm (I) takes up the bending moment due to tangential force and prevents carriage lift-off during operation.

With the above system, the lathe experiences only the axial and tangential components of force (both relatively small). The large, radial component of force is taken up by the tooling assembly itself.

This experimental setup was successful in accommodating the forming loads without deflecting significantly. The shear forging and support roller arm could each be expected to deflect radially away from the workpiece and die by approximately 0.25mm (0.010 in.), under maximum operating conditions, for a total deviation, from the preset reduction, of 0.50 mm (0.020 in.). The large deflections of up to 6 mm ($\frac{1}{4}$ in.) previously encountered, due to the lack of support rigidity between the steady rest and the lathe bed, were thus largely eliminated.

In addition, a complete set of rollers was fabricated (Fig. 47) for shear forging, rib forging, and for blending the rib-forged section to the shear-forged section.

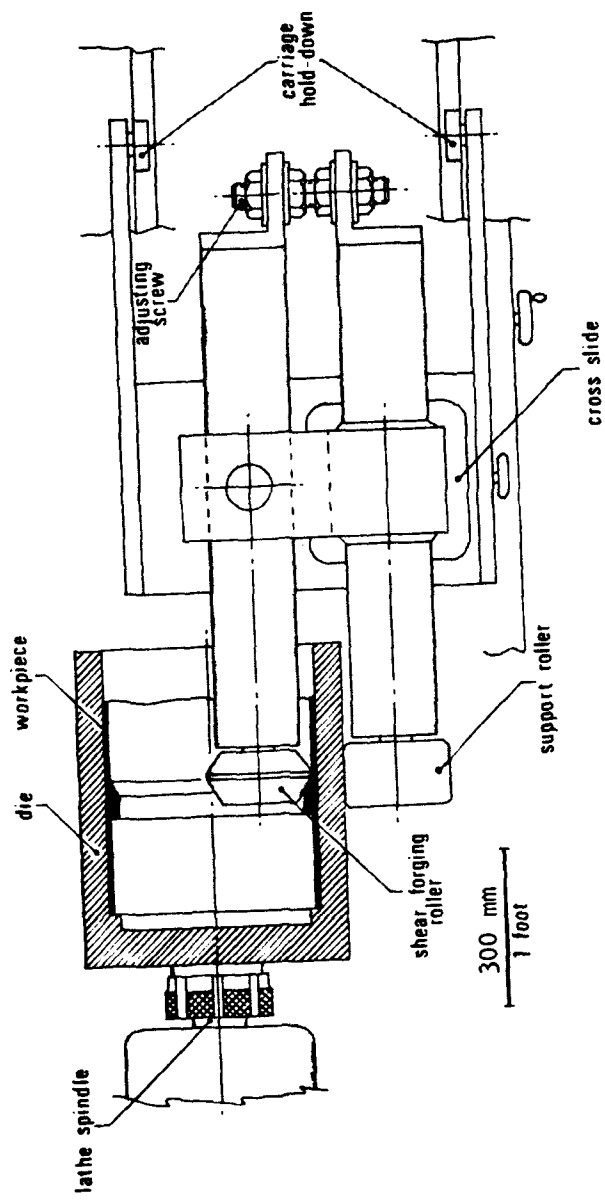


Figure 45. Improved tooling design for internal shear forging.

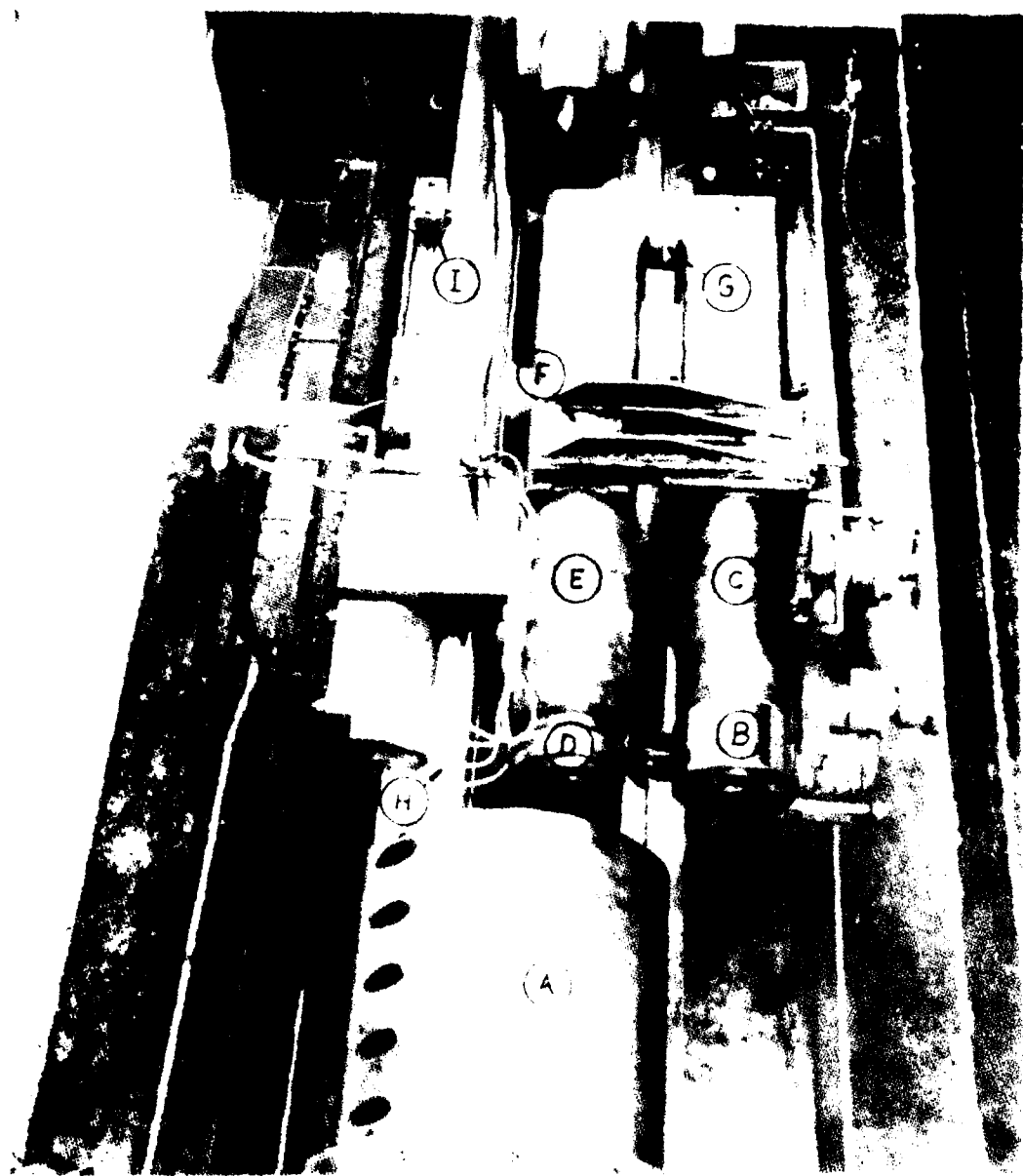
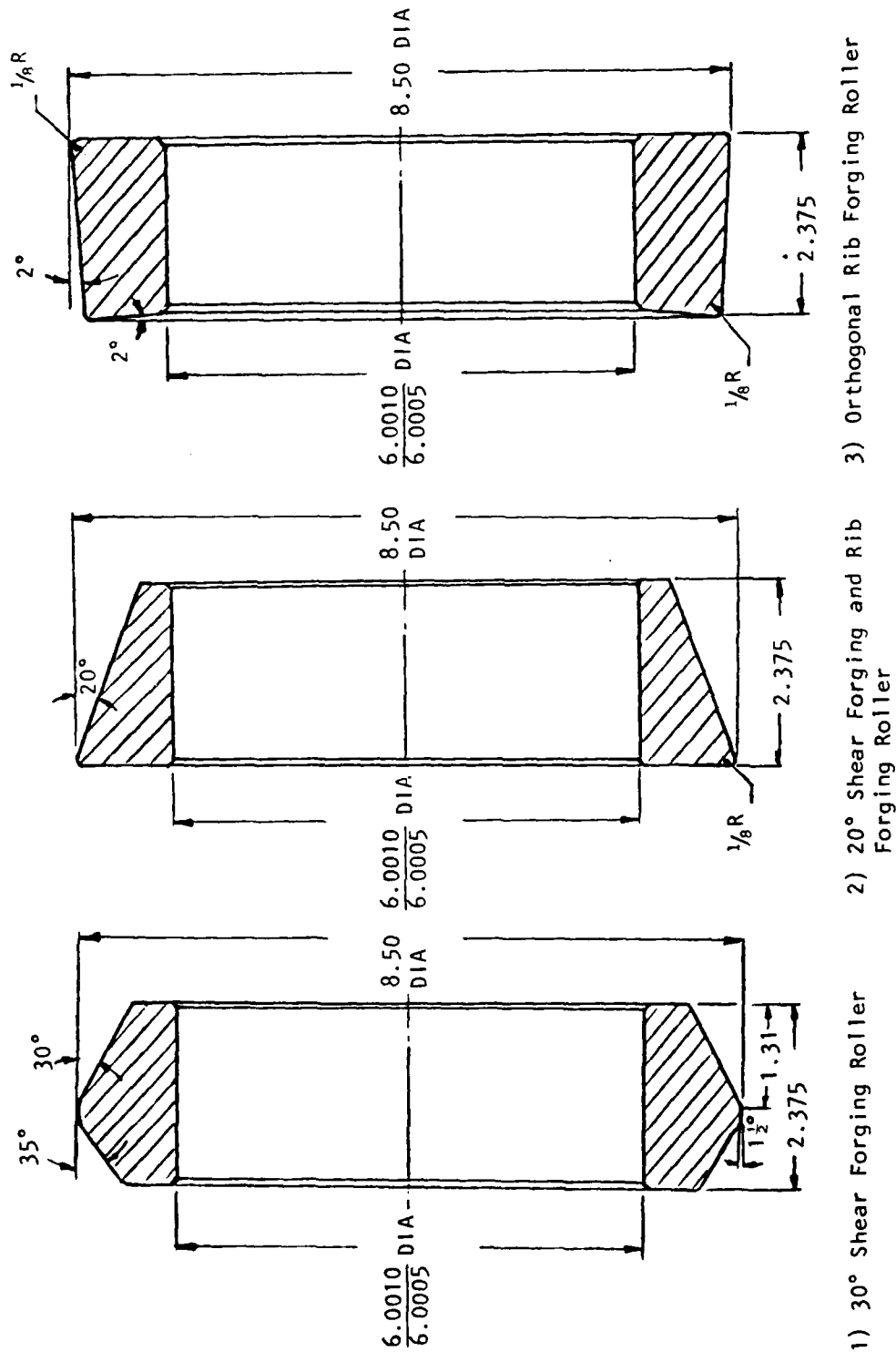


Figure 46. Modified tooling for internal shear forging,
assembled in LeBlond 2516 engine lathe.



Notes:

- All ID Chamfers are $1/16 \times 45^\circ$
- Grind All Surfaces
- Polish After Grinding, All Surfaces Except ID to 2 Microinches RMS.

DWG. No. M6013-28
Modified Rollers
For Shear Forging
No. REQ: 1 ea
Material: D2 Tool
Steel
HRC 60-62

Figure 47. Modified rollers for internal shear forging.

6. INTERNAL SHEAR FORGING OF SUBSHELLS

6.1 PROCESS DESCRIPTION

Using the modified tooling described in the foregoing section, thick-walled 2014-0 rings were successfully shear forged into thin-walled internally ribbed tubes. Thermomechanical treatments were evaluated by introducing cold work at various stages of the precipitation hardening cycle for the workpiece material. The processing sequence is shown for one TMT cycle in Figure 48.

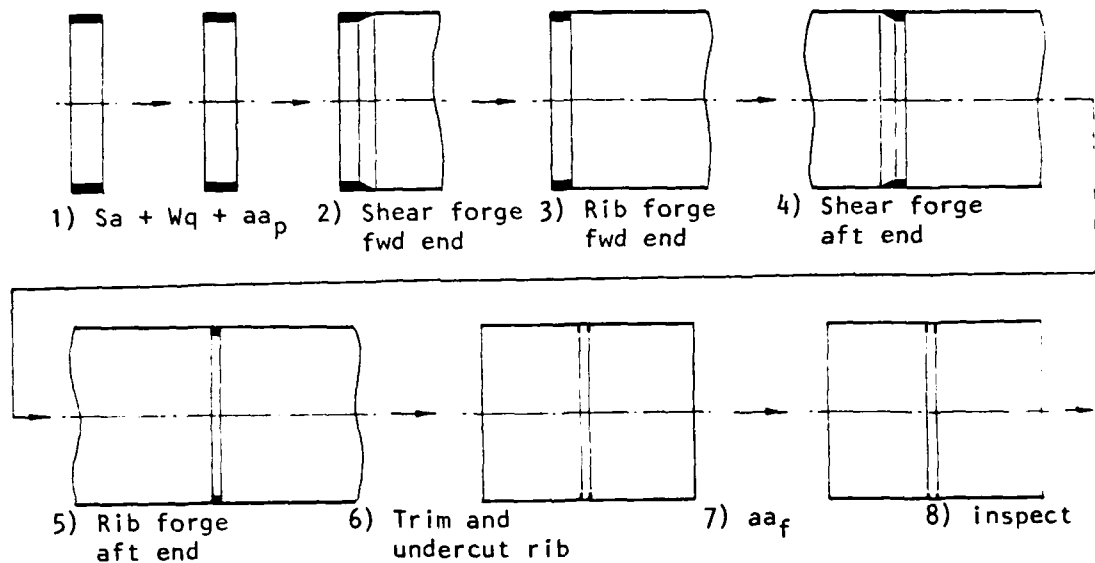


Figure 48. Process elements in internal shear forging of 2014 Al subshells.

The deformation processes involved are illustrated schematically in Figure 49. Lubrication during the initial passes--which were made at approximately 177°C (350°F)--was accomplished using a graphite (Aquadag) spray on the workpiece, Figure 50. Figure 51 shows the process of ribs forging to orthogonalize the ribs. Solution treatment was accomplished in a Globar-heated electric furnace (Figure 52) at 55°C (930°F). The

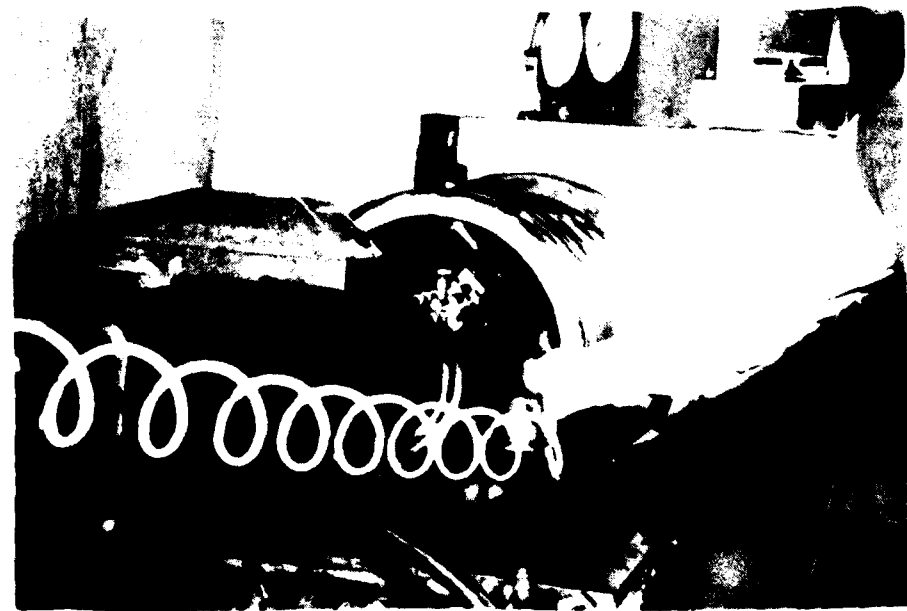
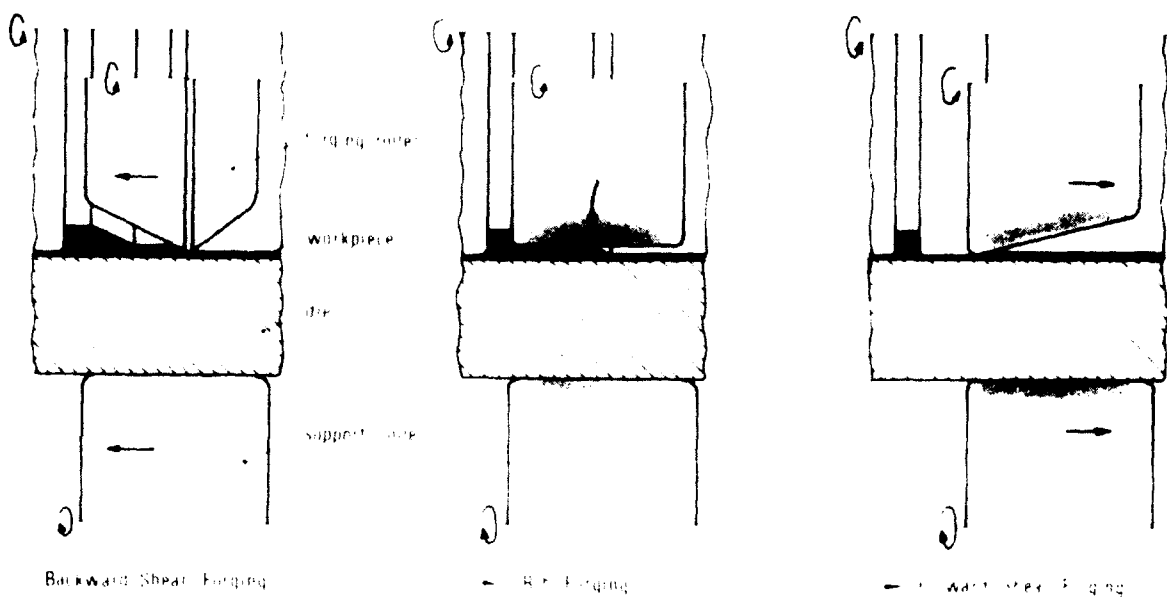


Figure 50. Graphite spray lubrication during initial warm deformation in internal shear forging.



Figure 51. Adjusting screw being turned for rib forging.



Figure 52. Intermediate tube wrapped in aluminum foil (to prevent radiant heating) and loaded in furnace for solution treatment.

final passes following solution treatment and different preaging treatments were made at room temperature (to prevent overaging) using a light oil for lubrication. Figure 53 shows the final, thermomechanically treated tube being removed from the die.



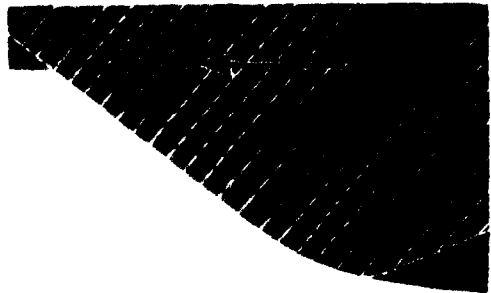
Figure 53. Thermomechanically treated, internally ribbed tube being removed from the die.

6.2 METAL FLOW

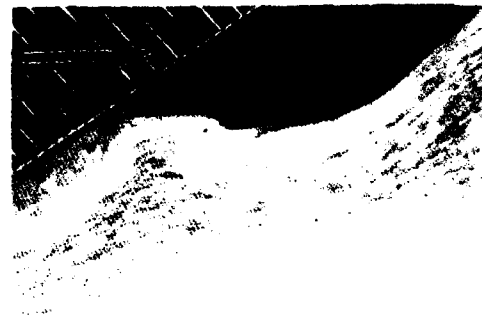
The various types of metal flow encountered in internal shear forging are shown in Figure 54. Figures 54a and 54b illustrate a near-uniform flow of metal under the roller (shown cross-ruled above the workpiece section) with no folding of metal ahead of the roller. This type of metal flow typically occurred after the first two or three passes, with gradual heating and increased plasticity of the workpiece enabling higher percent reductions to be taken. In the initial passes, the metal flow was usually less uniform because of loading limitations and insufficient percent reduction in the wall. An extreme case of nonuniform flow is shown in Figure 54c, with intense shearing of the



(a) Uniform flow



(b) Uniform flow



(c) Nonuniform flow with intense surface shear leading to surface folds



(d) Metal flow in rib forging

Figure 54. Low-magnification photomicrographs showing metal flow in internal shear forging.

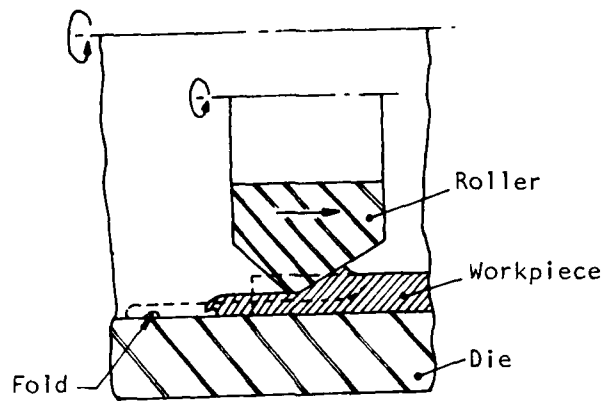
surface layers of metal, and formation of dead-metal zones, folds, and laminations. In contrast, the rib forging operation that was performed to orthogonalize the rib section produced uniform flow of metal under the roller (Figure 54d) despite some shaving of the vertical face of the rib due to friction.

Numerous structural defects were observed in the early trials, which had to be studied and resolved. Their causes and remedies are discussed below, in decreasing order of the frequency of occurrence of such defects.

a) Folds on Outside Surface. The compressive stress field in the deformation zone is concentrated directly under the shear forging roller since the area of contact is limited in the case of the roller-workpiece interface. At the workpiece-die interface, the same compressive load is distributed over a larger contact area. The end result is that the majority of plastic deformation is confined to the workpiece layers immediately below the workpiece, especially for low initial reductions.

Consequently, the axial elongation of the part is more pronounced, in the early passes, in the inside surface layers of the workpiece, resulting in a bulging out of ID material, Figure 55. During subsequent passes, the bulge produced on the ID is folded back to the OD (die surface) resulting in a discontinuity on the outside surface of the shear forged part. Fortunately, this fold is generally formed at the tail end of the final skin and is removed by trimming about 50 mm (2 in.) off either end of the finished component.

b) Laminations on Inside Surface. Another effect of inhomogeneous deformation is the buildup observed ahead of the roller. This in itself is usually not detrimental to the part. However, in extreme cases or when rib forging is performed to square the rib section, previously built-up layers become flattened to produce foil-like laminations on the ID surface, Figure 56.



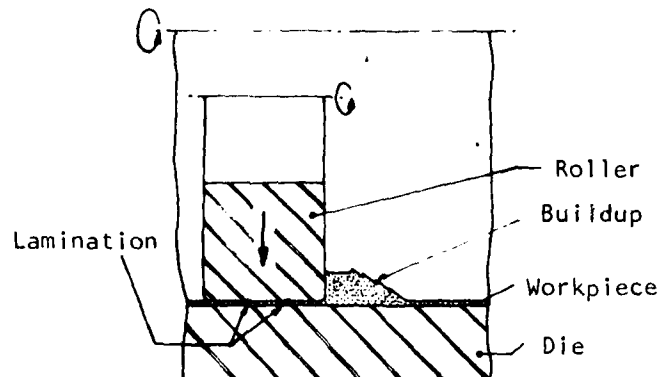
(a)



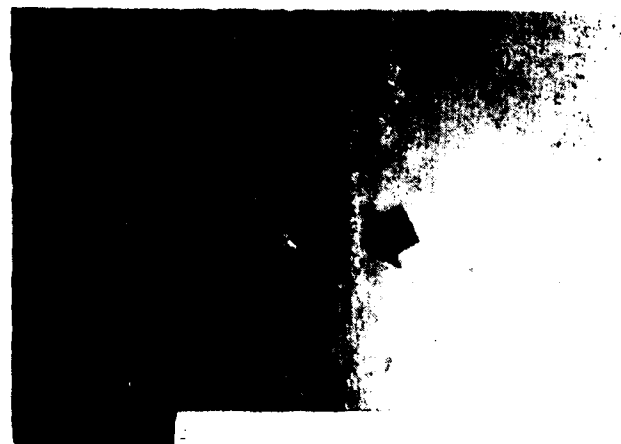
Neg. No. 52615

(b)

Figure 55. Fold produced due to inhomogeneous deformation, shown schematically (a) and on an actual part (b).



(a)



Neg. No. 52614

(b)

Figure 56. Lamination defect, caused on the ID surface during rib forging by foldover of buildup from previous passes, shown schematically (a) and on an actual part (b).

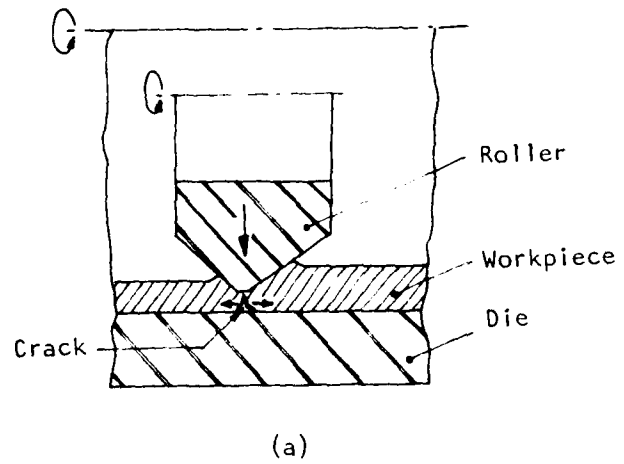
This can be avoided (a) before the fact by undertaking a cleanup cut on the rib area prior to rib forging, or (b) after the fact by removing the laminations with emery cloth and following up with a final shear forging pass.

c) Cracking. Cracking of the outside surface of the wall, Figure 57 is due to secondary tensile stresses in the axial direction generated by the wedge action under the roller. This phenomenon is usually evident when the roller is plunged into the material radially, when the material is formed cold or in the T6 temper, when the clearance angle on the roller land is low, or when deep impressions are left by the turning operation during preform preparation which later act as stress raisers.

d) Buckling. In backward shear forging, buckling ahead of the roller is the result of high axial load which, in turn, is caused by high reduction and feed rate, Figure 58. In addition, for the particular case of internal shear forging, buckling was also observed in the reduced section behind the roller (Figure 58). This is attributed to diametral expansion of the reduced section within a rigid die, which sets up a compressive hoop stress in the thin skin and causes the latter to buckle.

e) Voids. In one instance, examination of a finished part revealed a through-hole in the reduced wall section, Figure 59. The cause of this void formation is not clear. Two reasons proposed are the presence of a hard inclusion in the preform of greater size than the final thickness of the part, and the entrapment--ahead of the roller or on the die--of shaved particles of buildup material or other forms of wear debris.

Shaving of metal by the wiping action of the roller is not discussed separately since it is not believed to produce any structural damage by itself. Nevertheless, it can be detrimental to the ID surface unless the shaved particles are periodically removed from the vicinity of contact between the roller and the workpiece.



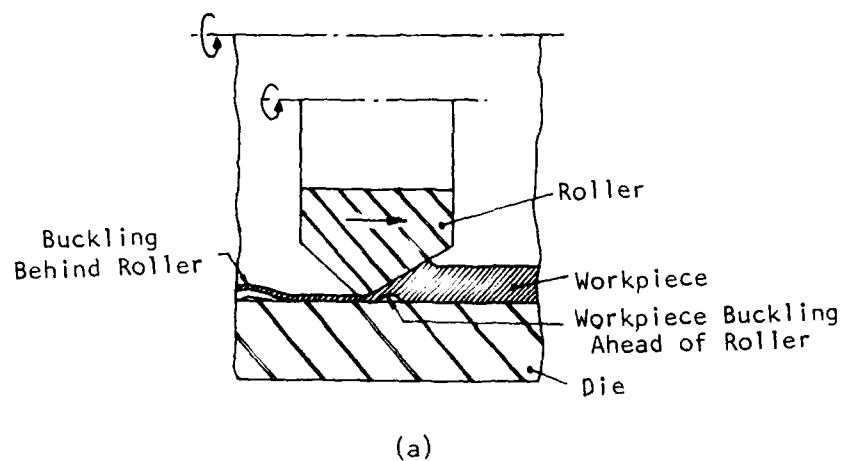
(a)



Neg. No. 52613

(b)

Figure 57. Cracking of wall OD from secondary tensile stresses due to high radial feed, low temperature, inadequate roller clearance, and rough machining marks on preform OD, shown schematically (a) and on an actual part (b).

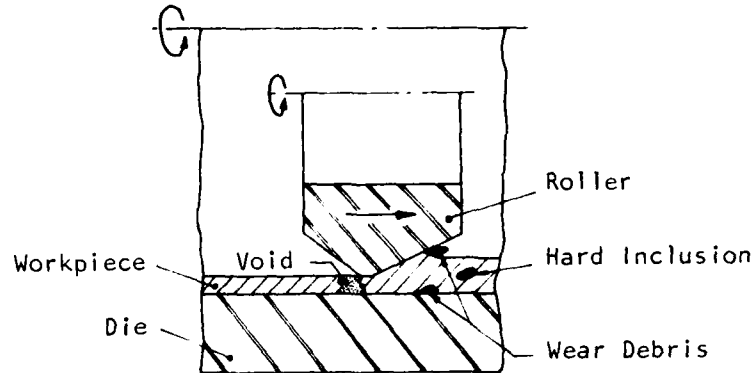


(a)



(b)

Figure 58. Buckling of thick wall ahead of roller and thin wall behind roller due to heavy reduction and feed rate in final pass, shown schematically (a) and on an actual part (b).



(a)



Neg. No. 52610

(b)

Figure 59. Void observed in thin wall in one case, attributable to hard inclusion or entrapment of wear debris in final pass, shown schematically (a) and on an actual part (b).

6.3 SHEAR FORGING OF 2014 Al AND 2024 Al SUBSHELLS

In addition to 2014 Al (program alloy), a few tests were conducted with 2024 workpieces fabricated from plate by roll-bending and welding. In contrast, all the 2014 Al workpieces were ring-rolled to provide a weld-free structure.

The strength, elongation, and hardness values for 2014 and 2024 aluminum alloys after internal shear forging are given in Table 6. The as-formed skin showed decreasing strength with increasing wall reduction. This is not the expected result of softening during mechanical working, since the preform was fully annealed to begin with and the processing was conducted below the recrystallization temperature. However, it may be an evidence of the Bauschinger effect, since the tensile tests reversed the polarity of the stress field present during forming.

The strength levels after heat treatment to the T6 condition showed no significant effect of deformation behavior, the yield and tensile strengths being in accordance with handbook data for these materials.

Surface roughness measurements on parts produced by internal shear forging (Table 7) indicate that the surface finish on the ID (20-65 μ in. AA) is consistent with standard cold rolling practice, Figure 60.

The ID finish is dictated by the finish on the roller (3 μ in.), and by the feed rate and roller geometry. For the case of forward shear forging (samples 9 and 10), no land was provided on the roller, resulting in a rough surface (150 μ in. AA).

The finish on the OD is generally a replica of the die contact surface. In the present case, the die was finish-turned to approximately 16-32 μ in. AA, but subsequent use resulted in localized roughening to 32-63 μ in. Consequently, the OD surface finish is seen in Table 7 to vary from 15 to 80 μ in. AA.

In addition, entrapment of graphite lubricant on both surfaces of the workpiece could be responsible for considerable scatter in surface roughness measurements, as seen in Table 7.

TABLE 6. MECHANICAL PROPERTIES OF INTERNALLY SHEAR FORGED SAMPLES

Identifi- cation	No.	ISF Reduction, %	Yield Strength, MPa (ksi)	UTS, MPa (ksi)	Elongation in 25 mm, %	Hard- ness, HRB
2014-F ^a	1 ^c	0	261 (37.9)	352 (51.1)	8.0	33
	2 ^d	90	208 (30.2)	270 (39.1)	10.0	28
2014-T6 ^b	3 ^c	0	439 (63.6)	492 (71.3)	11.0	84
	4 ^d	90	419 (60.8)	521 (75.5)	10.0	82
2024-F ^a	5 ^e	0	197 (28.5)	304 (44.1)	11.0	45
	6 ^d	93	188 (27.3)	263 (38.1)	12.0	30
	7 ^d	95	179 (25.9)	230 (33.4)	5.0	22
2024-T6 ^b	8 ^e	0	385 (55.8)	481 (69.8)	11.0	85
	9 ^d	93	350 (50.8)	439 (63.6)	14.0	78
	10 ^d	95	377 (54.7)	456 (66.1)	8.0	78

Notes:

1. Handbook properties are as follows:
 2014-T6: 414 MPa (60 ksi) yield; 483 MPa (70 ksi) UTS;
 13% elongation
 2024-T6: 393 MPa (57 ksi) yield; 476 MPa (69 ksi) UTS;
 10% elongation
2. Forming temperature was 150°-200°C in all cases.

^a Tested in as-internally shear forged condition.
^b Tested after solution annealing, water quenching, and artificial aging to the T6 temper.
^c Test direction was along the circumference of the internally shear forged tube; sample dimensions were 6.4 mm ($\frac{1}{4}$ in.) dia. x 25 mm (1 in.) gage length.
^d Test direction was along the length of the internally shear forged tube; sample dimensions were (as-forged thickness) x 6.4 mm width x 25 mm gage length.
^e Test direction was along the length of the internally shear forged tube; sample dimensions were 6.4 mm dia. x 25 mm gage length.

TABLE 7. SURFACE FINISH OF INTERNALLY SHEAR FORGED PARTS

No.	ISF Mode	Feed Spacing, mm (in.)	AA Surface Roughness, μm ($\mu\text{in.}$)		
			ID (axial)	OD (axial)	OD (circumf.)
1	Backward	2.54 (0.100)	0.5 (20)	0.8 (30)	--
2	Backward	1.91 (0.075)	1.7 (65)	1.3 (50)	--
3	Backward	1.52 (0.060)	1.0 (40)	0.9 (35)	--
4	Backward	2.03 (0.080)	0.5 (20)	1.1 (45)	2.0 (80)
5	Backward	1.52 (0.060)	1.1 (45)	1.4 (55)	--
6	Backward	1.27 (0.050)	0.5 (20)	1.5 (60)	1.3 (50)
7	Backward	2.54 (0.100)	0.9 (35)	1.1 (45)	1.5 (60)
8	Backward	2.16 (0.085)	0.5 (20)	1.8 (70)	--
9	Forward	0.89 (0.035)	3.8 (150)	0.5 (20)	0.4 (15)
10	Forward	0.64 (0.025)	3.8 (150)	1.0 (40)	1.9 (75)

Note: In all cases, the workpiece material was 2014 aluminum, internally shear forged at 150°-200°C, 50 rpm (1.0 m/s) speed, 0.13 mm/rev feed rate for final pass, and 1 mm final thickness.



Neg. 52616 $\frac{1}{4}$ Scale
Figure 60. Inside surface finish of part produced by ISF/RF.

6.4 THERMOMECHANICAL TREATMENT OF 2014 Al SUBSHELLS

Thermomechanical treatment (TMT) is a means of improving the properties of certain alloys by introducing plastic deformation into the heat-treatment cycle. The microstructural changes accompanying the process are different from those in conventional processing. Depending on the alloy and the nature of the TMT, this can result in improved tensile strength and elongation, better fatigue, creep, and wear resistance, and higher levels of fracture toughness and stress corrosion resistance.

Reviewing Soviet progress in this area, Azrin *et al.*⁴⁰ detailed the following findings for precipitation-hardenable aluminum alloys:

- 1) Plastic deformation accelerates the precipitation reaction in these alloys, due to the hereditary effect of prior deformation of subsequent precipitation, and also the dynamic effect of precipitation accompanying deformation. This leads to finer, more homogeneous precipitation than possible in conventional processing (without deformation).
- 2) In high-strength aluminum alloys, stress corrosion resistance can be enhanced by partially aging (artificially) the solutionized material prior to deformation, followed by final aging. Homogeneous precipitation occurs within the grains, by this form of double aging, at the expense of grain-boundary precipitation. In addition, continuous boundary precipitates are fragmented, resulting, overall, in improved resistance to grain-boundary fracture from stress corrosion.
- 3) In many aluminum alloy systems, TMT can lead to reduced strength from overaging as a result of the accelerated kinetics of the final aging operation. Higher overall properties have been obtained with Al-Cu-Mg, Al-Mg-Si, and Al-Mg-Zn systems when using a TMT sequence of solutionize, cold work, and age. The double-aging sequence of solutionize, age, cold work, and age has been applied successfully to the above alloy systems and also to Al-Cu-Li alloys. The double-aging sequence generally leads to better resistance to stress corrosion cracking. In many cases, double aging also produces an enhanced rate of work hardening during deformation to result in dramatic increases in strength after final aging.
- 4) In some alloys, fracture toughness is enhanced due to a distorted grain-boundary structure resulting from TMT; this structure changes the mode of fracture from intergranular to transgranular.

Six different TMT cycles were evaluated in this program (Figure 61). They differed from one another primarily in the stage of the precipitation-hardening sequence in which cold work was introduced. In addition, the time and temperature of preaging (after solution treatment, before cold work) was varied, wherever possible, to investigate the precipitation kinetics to a limited extent.

In all cases, the starting material was a ring-rolled and fully annealed ring of 2014 aluminum (Figure 62). The microstructures resulting from the various TMT cycles are shown in Figures 63-68. In general, cold work following solution treatment is seen to fragment the grains, with the most dramatic fragmentation occurring when cold work is imposed on a fully aged, T6 structure.

The tensile properties measured under these conditions are given in Tables 8 and 9. On the basis of the data shown in Table 8, cycle 6--which is a double-aging TMT cycle--was selected for production of the deliverable subshells. Two other cycles--cycle 2 (T6) and cycle 4 (T9)--were selected for preparation of samples for further testing by MIRADCOM.

In general, cold work appears to hasten the precipitation-hardening kinetics of 2014 aluminum (Table 9). The final aging temperature thus has to be lower than for conventional artificial aging to the T6 condition to avoid overaging.

The tensile test data presented in Tables 8 and 9 indicate that the response of 2014 aluminum to thermomechanical treatment is only marginal insofar as tensile properties are concerned. Although higher strengths have been attained here than in conventional T6 heat-treatment, it has been at the expense of ductility (tensile elongation). The effect on fatigue strength, fracture toughness, and stress corrosion cracking would be evaluated by MIRADCOM, if warranted, external to this program.

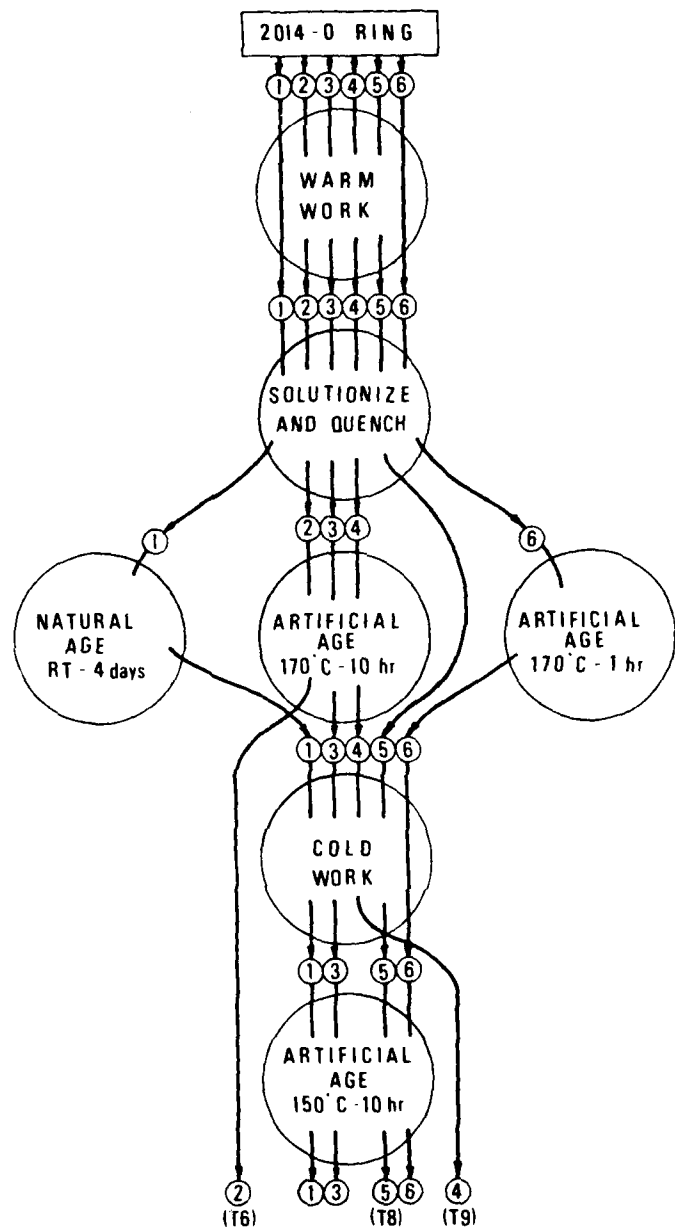
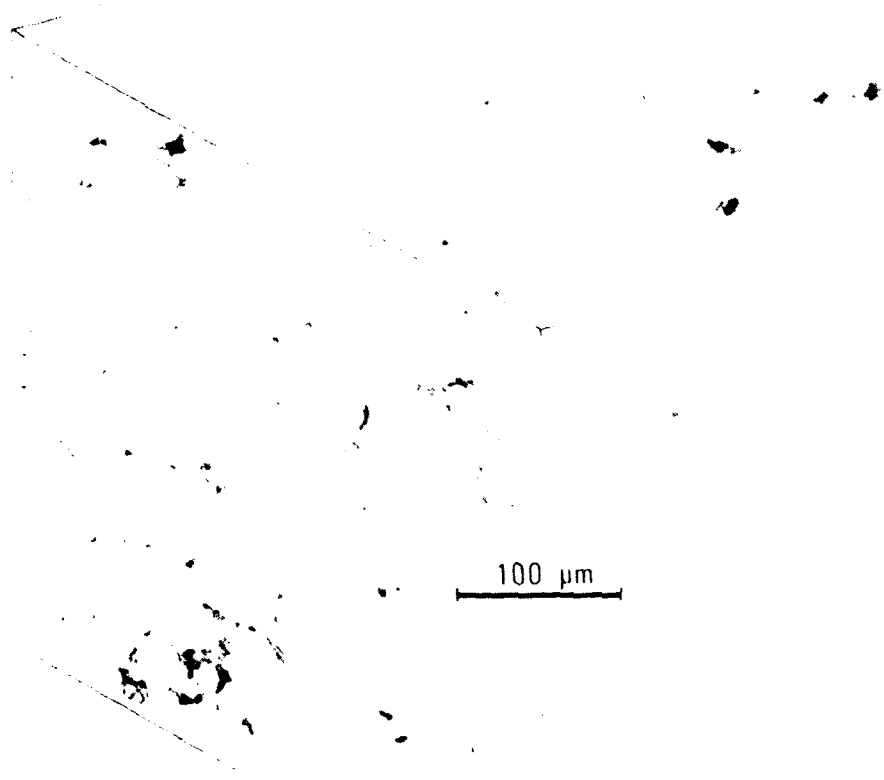


Figure 61. Thermomechanical treatment (TMT) cycles evaluated during internal shear forging of 2014 aluminum.



Neg. Nos. (A) 53047
(T) 53046
(R) 53045

T * A
R

Figure 62. Optical photomicrographs of 2014-0 aluminum specimen prior to internal shear forging.



Neg. Nos. (A) 53052
(T) 53061
(R) 53060

T
A
R

Fig. 63. Optical photomicrographs of internally shear forged 2014 aluminum specimen after cycle 1: Warm working, solutionizing and quenching, natural aging to T4 condition, cold working 40%, and artificial aging at 150°C-10 hr.

AD-A102 848

IIT RESEARCH INST CHICAGO IL
INTERNAL SHEAR FORGING PROCESSES FOR MISSILE PRIMARY STRUCTURES--ETC(U)
JUL 81 S RAJAGOPAL, S KALPAKJIAN
UNCLASSIFIED IITRI-M06013-33

F/G 20/11

DAAK40-78-C-0264

NL

2 n 2
AD
A102 848

END
DATE
FILED
9-81
OTIC

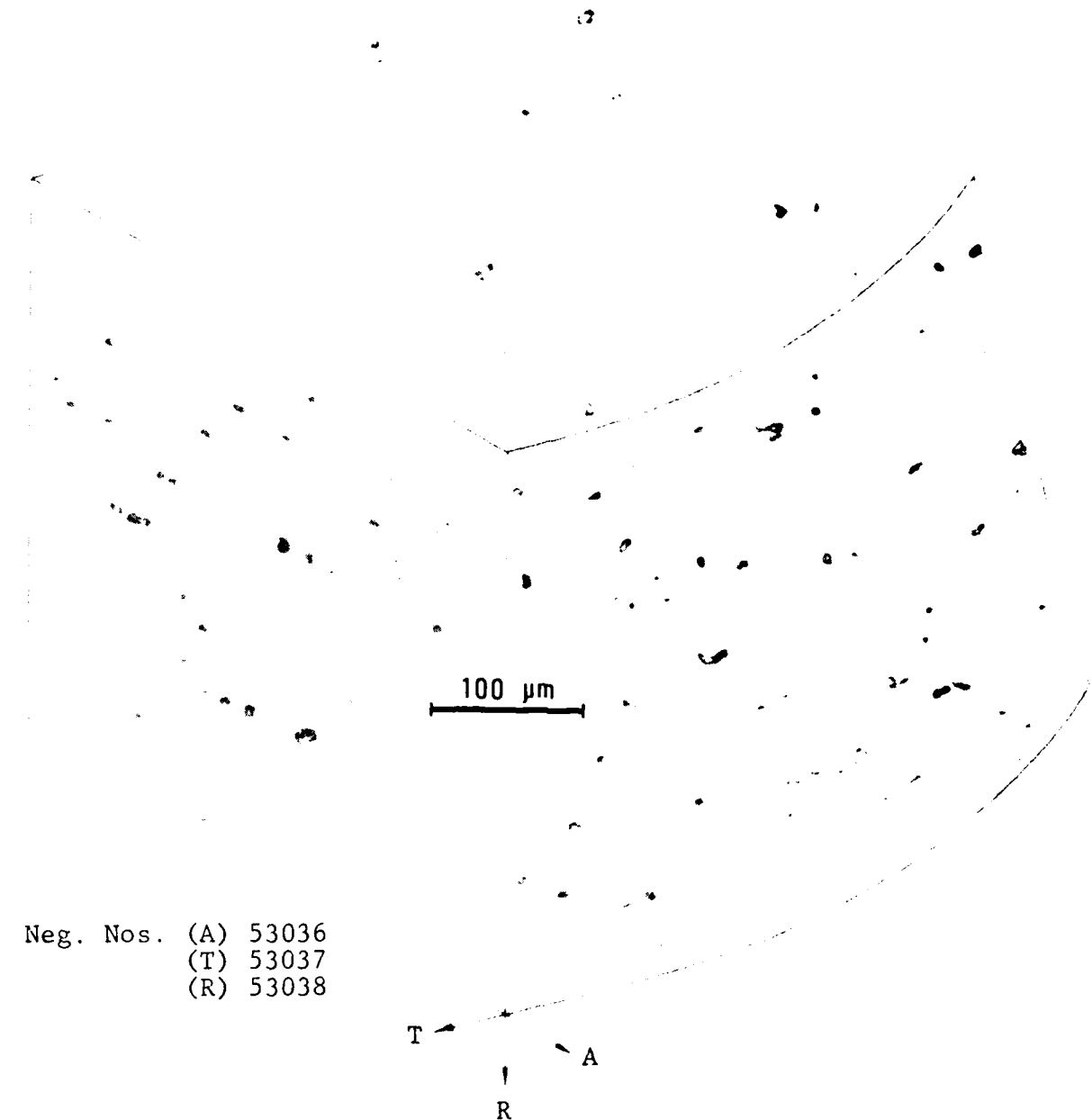


Figure 64. Optical photomicrographs of internally shear forged 2014 aluminum specimen after cycle 2: Warm working, solutionizing and quenching, and artificial aging at 170°C -10 hr to T6 condition.

Neg. Nos. (A) 53042
(T) 53043
(R) 53044

T
A
R

Figure 65. Optical photomicrographs of internally shear forged 2014 aluminum specimen after cycle 2: Warm working, solutionizing and quenching, artificial aging at 170°C -10 hr (T6), cold working 20%, and artificial aging at 150°C -10 hr.

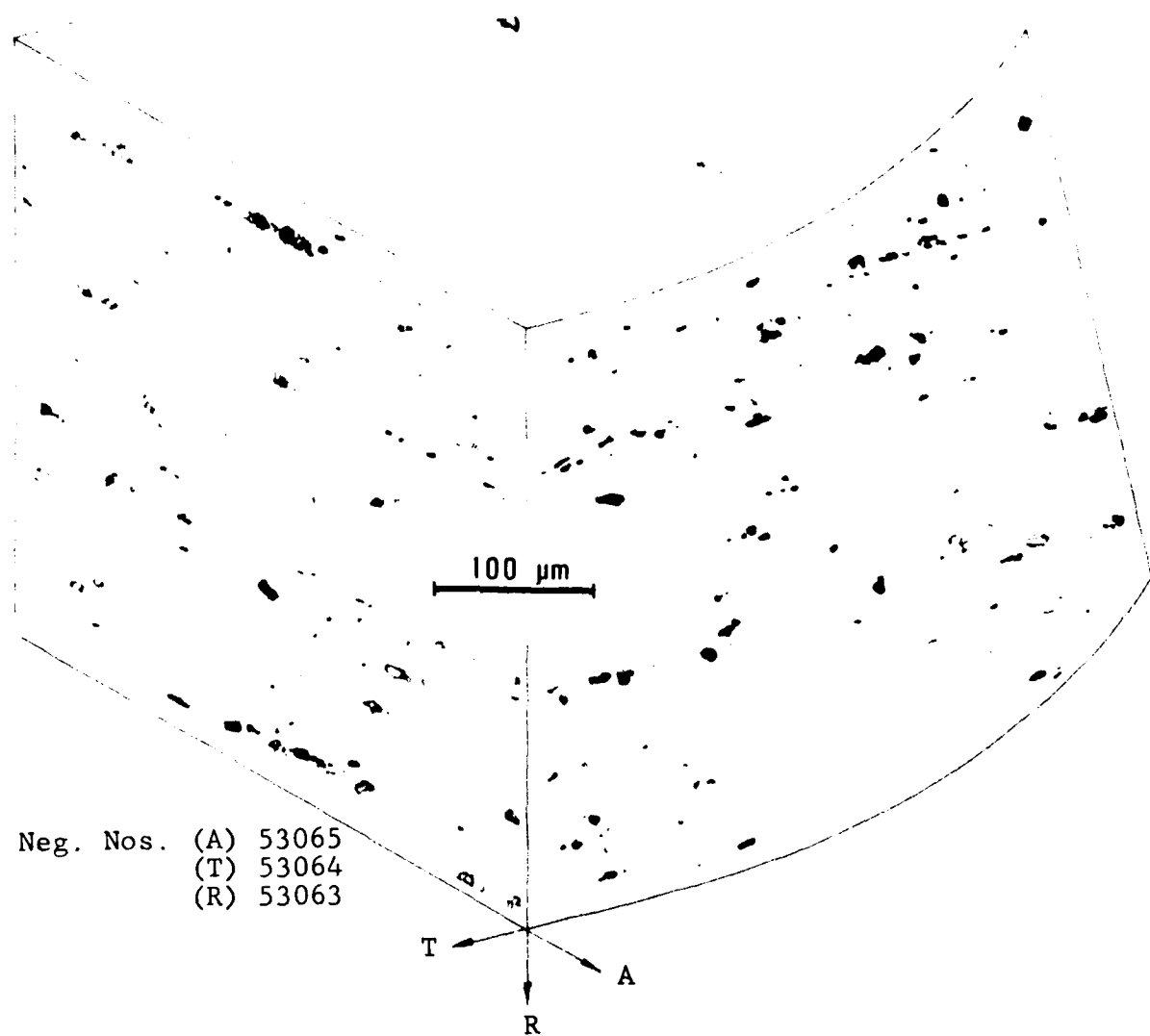


Figure 66. Optical photomicrographs of internally shear forged 2014 aluminum specimen after cycle 4: Warm working, solutionizing and quenching, artificial aging at 170°C -10 hr (T6), and cold working 20% to T9 condition.

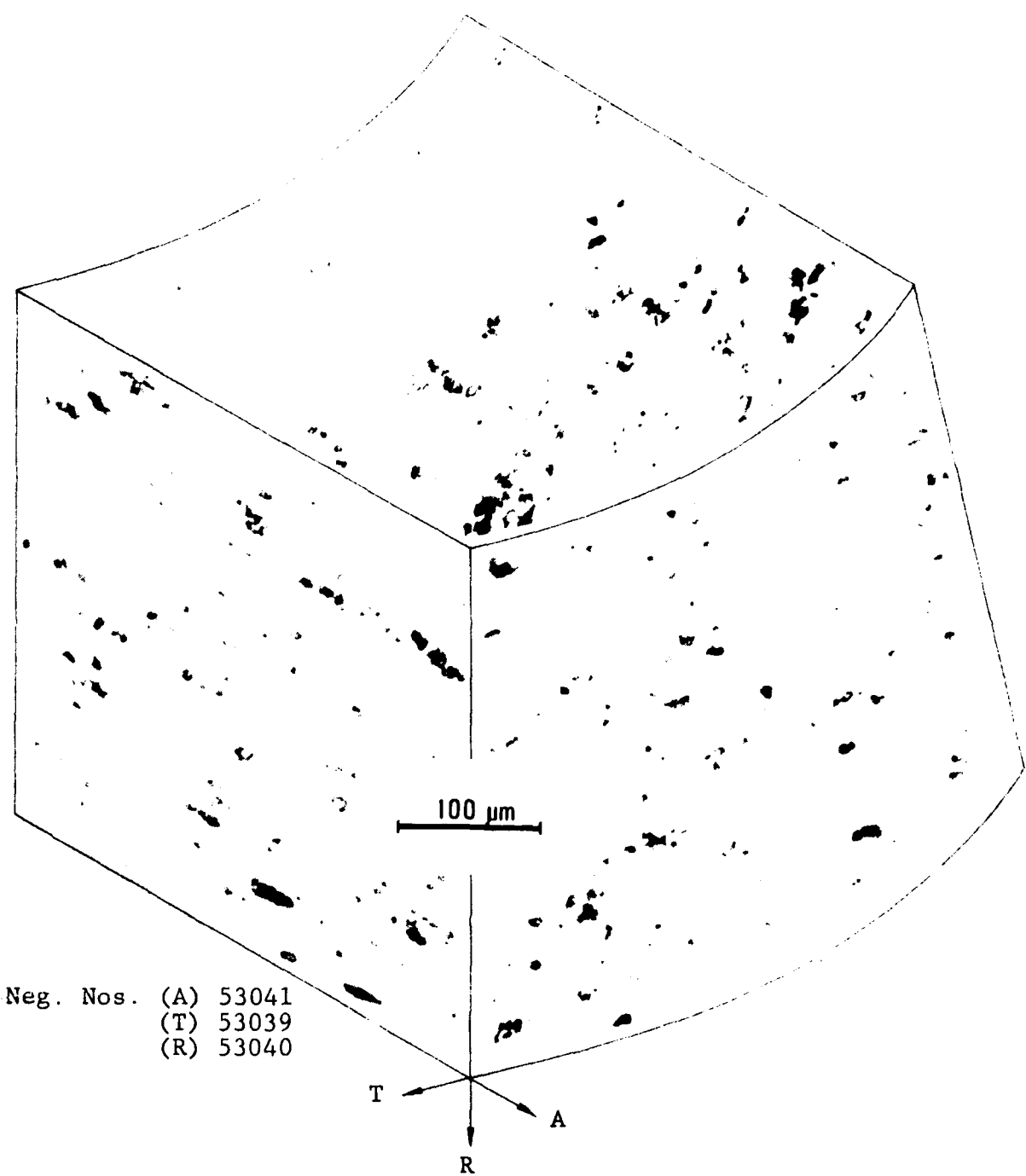


Figure 67. Optical photomicrographs of internally shear forged 2014 aluminum specimen after cycle 5: Warm working, solutionizing and quenching, cold working 30%, and artificial aging at 150°C -10 hr to T8 condition.



100 μm

Neg. Nos. (A) 53059
(T) 53058
(R) 53057

T A
R

Figure 68. Optical photomicrographs of internally shear forged 2014 aluminum specimen after cycle 6: Warm working, solutionizing and quenching, artificial aging at 170°C -1 hr, cold working 10%, and artificial aging at 150°C -10 hr.

TABLE 8. TENSILE PROPERTIES OF INTERNALLY SHEAR FORGED 2014 ALUMINUM ALLOY AFTER DIFFERENT THERMAL-MECHANICAL CYCLES

Cycle*	Test Direction**	Yield Strength		Tensile Strength		Elongation in 25 mm, %
		MPa	ksi	MPa	ksi	
1	A	394	57.1	418	60.6	11
	T	404	58.6	434	62.9	9
2	A	442	64.1	458	66.4	8
	T	423	61.4	451	65.4	7
3	A	513	74.4	518	75.1	5
	T	505	73.3	510	74.0	4
4	A	536	77.7	540	78.3	3
	T	506	73.4	507	73.5	2
5	A	359	52.0	424	61.5	8
	T	413	59.9	445	64.5	10
6	A	427	62.0	442	64.1	10
	T	445	64.5	456	66.2	6

Specimen Geometry: 6 mm width x 1 mm thickness x 25 mm gage length.

* Warm work 94%, solutionize (500°C-4 hr) and quench, followed by

- 1 - Natural age (T4), cold work (40%), and artificial age at 150°C-10 hr.
- 2 - Artificial age at 170°C-10 hr (T6).
- 3 - Artificial age at 170°C-10 hr (T6), cold work (20%), and artificial age at 150°C-10 hr.
- 4 - Artificial age at 170°C-10 hr (T6), and cold work 20%, (T9).
- 5 - Cold work (30%) and artificial age at 150°C-10 hr (T8).
- 6 - Artificial age at 170°C-1 hr, cold work (10%), and artificial age at 150°C-10 hr.

** A - Axial direction of tube.

T - Tangential direction of tube.

TABLE 9. EFFECT OF FINAL AGING TREATMENT ON TENSILE PROPERTIES
OF 2014 ALUMINUM ALLOY

Cycle*	Final Aging	Test Direction**	Strength,		Tensile Strength,		Elongation in 25 mm, %
			MPa	ksi	MPa	ksi	
1	150°C-2 hr	A	363	52.7	419	60.8	12
		T	394	57.1	430	62.4	8
	150°C-10 hr	A	394	57.1	418	60.6	11
		T	404	58.6	434	62.9	9
3	170°C-2 hr	A	352	51.1	393	57.0	6
		T	397	57.6	425	61.7	7
	170°C-10 hr	A	343	49.8	387	56.1	9
		T	422	61.2	434	62.9	5
5	150°C-2 hr	A	436	63.2	492	71.3	3
		T	473	68.6	484	70.2	6
	150°C-10 hr	A	513	74.4	518	75.1	5
		T	505	73.3	510	74.0	4
6	170°C-2 hr	A	493	71.5	503	72.9	3
		T	499	72.3	509	73.8	5
	170°C-10 hr	A	483	70.0	496	72.0	4
		T	474	68.8	483	70.1	4
6	150°C-2 hr	A	357	51.8	423	61.4	9
		T	369	53.5	428	62.1	12
	150°C-10 hr	A	359	52.0	424	61.5	8
		T	413	59.9	445	64.5	10
6	170°C-2 hr	A	345	50.0	432	62.6	9
		T	414	60.0	445	64.6	9
	170°C-10 hr	A	419	60.7	425	61.6	4
		T	447	64.8	451	65.4	6

Specimen Geometry: 6 mm width x 1 mm thickness x 25 mm gage length.

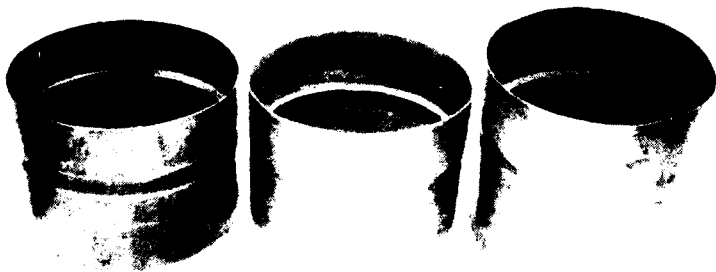
* Warm work 94%, solutionize (500°C-4 hr) and quench, followed by
 1. Natural age (T4), cold work (40%), and artificial age at 150°C-
 150°C-10 hr.
 3. Artificial age at 170°C-10 hr (T6), cold work (20%), and
 artificial age at 150°C-10 hr.
 5. Cold work (30%) and artificial age at 150°C-10 hr (T8).
 6. Artificial age at 170°C-1 hr, cold work (10%), and artificial
 age at 150°C-10 hr.

6.5 PROCESSING OF DELIVERABLE SUBSHELLS

6.5.1 Deliverable Items

Three deliverable subshells were processed according to the schematic shown earlier in Figure 48. This involved shear forging (170°C), rib forging (170°C), solutionizing and quenching, artificial preaging at 170°C-1 hr, shear forging (cold) by 10%, final artificial aging at 150°C-10 hr, and trimming to size. In addition, the skins of an additional subshell section were processed by T6 and T9 treatments and delivered to MIRADCOM for metallurgical and mechanical testing.

The three intact subshells are shown in Figure 69.



Neg. No. 53314

0.08x

Figure 69. Deliverable subshells, internally shear forged with thermomechanical treatment.

6.5.2 Residual Stresses

It was observed that internal shear forging with TMT--with the final passes performed cold on a preaged structure--resulted in considerable residual stresses. These stresses were either nonexistent or not apparent when shear forging annealed parts at warm temperatures.

Figures 70 shows one manifestation of the residual stresses remaining in the subshell after processing: departure from circular to hexagonal profile at some distance away from the reinforcing presence of the central rib. In one case, when an axial slit was made in the thermomechanically processed subshell, it coiled up into a spiral (Figure 71)--further evidence of residual stresses being present.

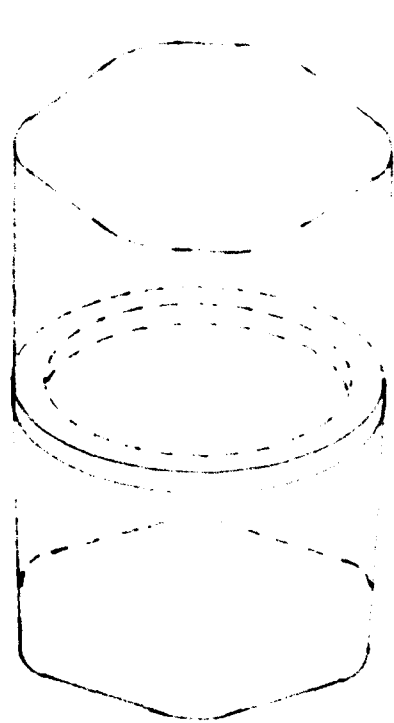
6.5.3 Thin Rib Generation

The target component depicted earlier in Figure 1 was intended to be internally shear forged leaving the central region as a single, thick rib. Grooving the thick rib in a lathe setup would then generate two separate, thin ribs. However, in producing the deliverable subshells, it was not possible to machine the rib to the desired specifications, for the reason given below.

The shear forging die was designed as a split (two-piece) construction,* held together by tangential bolts, to facilitate part removal after forming. Under load, the two-piece assembly was progressively distorted (and the bolts stretched) to result in an oval die and, hence, subshells with approximately 1.6 mm (1/16 in.) ovality.

It was decided not to machine the ribs so as to avoid the risk of breaking through the skin and rendering the subshells unusable.

*The experiments showed that a split die is not necessary and that by reverse feeding the roller, the part can be forcibly extracted from the die. A strong, rigid, single-piece die could thus be used to eliminate ovality and rib machining problems.



(a)

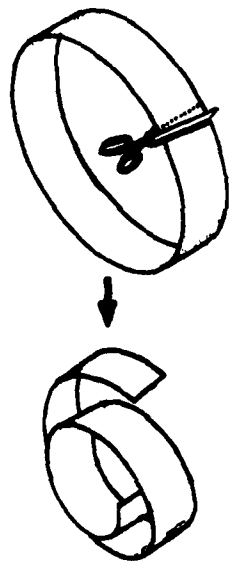


(b)

Neg. No. 53315

0.15X

Figure 70. Subshell distortion caused by residual stresses from internal shear forging of preaged material, shown schematically (a) and on an actual part (b).



(a)



(b)

Neg. No. 53317

0.2X

Figure 71. Observation of residual stresses by cutting a thermomechanically processed subshell, shown schematically (a) and on an actual part (b).

7. PRODUCTION REQUIREMENTS AND COSTS

This section details the equipment and tooling requirements for internal shear forging of thermomechanically treated 2014 aluminum sub-shells in production, the cycle time and production rates anticipated, and the cost benefits of implementing this technology in production.

7.1 EQUIPMENT AND TOOLING

The capital equipment for internal shear forging consists primarily of one or more heat-treating furnaces and one or more heavy-duty engine lathes or, preferably, spinning lathes. The quantity of each of these items would be determined by the cycle time and the rate of production desired. Tooling for internal shear forging would be as described earlier in Section 5, modified as necessary to suit the particular spinning machine used. Additional items include a lubricant spray system, and oxyacetylene heating system (optional) and material handling equipment.

An annual requirement of 2000 parts calls for one spinning lathe (\$200,000) and three heat-treating furnaces (\$300,000) for solutionizing, preaging, and final aging. The total investment in implementing the new technology in place of the current process is estimated to be \$1,000,000. As seen later, the annual return on this investment is expected to be \$6.86 per dollar invested, for a payback period of 1.7 months.

The shear forging die,*rollers, support members, and other items of tooling are expected to cost \$100,000 including rework and replacement parts for one year's production. Amortization over 2000 parts will result in a tooling add-on-cost of \$50 per part.

The cycle time, standard labor hours per part, and the total cost per part are discussed below.

*As discussed earlier in Section 6.5.3, the production die would be built as a single-piece unit to eliminate the problem of the distortion and resulting part ovality. All other items of tooling will be, in principle, similar to the internal shear forging tooling described in Section 5.4. Engineering drawings for these components are available at IITRI (Ref. IITRI-M06013).

7.2 PRODUCTION PROCESS SEQUENCE

Internal shear forging of 2014 aluminum subshells with thermo-mechanical treatment can be divided into eight process elements (Figure 48):

1. solution anneal, water-quench, and partial artificial age (sa + wq + aap)
2. shear forge forward end
3. rib forge forward end
4. shear forge aft end
5. rib forge aft end
6. trim and undercut ribs
7. final artificial age (aa_f)
8. inspect.

7.3 STANDARD HOURS FOR SUBSHELL PRODUCTION

The standard hours per subshell will be computed on the basis of a throughput time of two hours per subshell, i.e., a production rate of 0.5 subshells per hour.* The eight operations listed above would be conducted in four stations:

1. heat treatment station (2-man crew)
2. spinning lathe station (2-man crew)
3. machining station (1-man crew)
4. inspection station (1-man crew).

The standard hours per subshell will thus be 2 hours x 6 men = 12 man-hours. This number must now be verified against the actual throughput capability of each station.

*On a two-shift basis, this would satisfy an annual requirement of 2000 subshells.

7.3.1 Heat Treatment Station

The estimated standard hours for heat treatment are 2 hours x 2 men = 4 man-hours. This is a conservative estimate, as demonstrated below:

Furnace	Time at Temp., hr	Through-put Time, hr	Minimum Furnace Capacity, subshells	Actual Standard Hours for Loading- Unloading
1 (Solutionizing)	4	2	2	0.50
2 (Preaging)	1	2	1	0.25
3 (Final aging)	10	2	5	<u>1.25</u>
				2.00

In other words, a 2-man crew can easily handle a throughput of 0.5 subshells/hr at the heat-treatment station for solutionizing, preaging, and final aging operations.

7.3.2 Spinning Lathe Station

At this station, a 2-man crew must shear forge and rib forge the forward and aft ends of the subshell. The standard hours estimated earlier were 2 hours x 2 men = 4 man-hours. Let us now verify that this is within the manpower capability.

a) Forward End Shear Forging--The operations involved in shear forging one end of the subshell are as follows:

Pass No.	Thickness, mm		Travel, mm		Time, min
	Start	Finish	Start	Finish	
(Position blank)	--	--	--	--	1.00
(Reset roller)	--	--	--	--	0.50
1	19.1	11.4	36	31	0.75
(Reset roller)	--	--	--	--	0.50
2	11.4	6.9	61	97	1.20
(Reset roller)	--	--	--	--	0.50
3	6.9	4.1	97	168	1.93
(Reset roller)	--	--	--	--	0.50
4	4.1	2.4	168	279	3.33
(Reset roller)	--	--	--	--	0.50
5	2.4	1.5	279	462	5.53
(Reset roller)	--	--	--	--	0.50
6	1.5	1.0	462	665	<u>9.13</u>
					25.87

Forward end shear forging, total time = 25.87 min/part

Standard hours per part with a 2-man crew = 0.86

b) Forward End Rib Forging--Rib forging is conducted by flattening the taper under the roller and following up with a final shear forging pass to obtain uniform wall thickness. The operations involved are:

Change roller - 5 min
 Flatten taper - 10 min
 Change roller - 5 min
 Shear forge - 10 min

Forward end rib forging, total time = 30 min/part

Standard hours per part with a 2-man crew = 1.00

c) Aft End Shear Forging--The partially forged subshell is now reversed inside the die to expose the hitherto undeformed wall to the shear forging roller. This is identical to forward and shear forging (item a) except that an additional one minute will be spent in removing the subshell from the shear forging die and reversing its position in the die. Thus,

Aft end shear forging, total time = 26.87 min/part
Standard hours per part with a 2-man crew = 0.90

d) Aft End Rib Forging--This is identical to forward end rib forging (item b) except that an additional one minute will be required for subshell removal after the operation. Thus,

Aft end rib forging, total time = 31 min/part
Standard hours per part with a 2-man crew = 1.03

e) Actual Standard Hours for Spinning Lathe Station--As a total of the time consumed in each of the preceding four operations, the floor-to-floor time at the spinning lathe station is 113.74 min or 1.9 hours per subshell, which is within the estimated 2 hours per subshell. The actual standard hours at this station will be 3.8 per subshell, which justifies the use of four standard hours per subshell in the economic analysis.

7.3.3 Machining Station

Having shear forged and rib forged the ring into a thin-walled shell, the ends must now be trimmed to size and a groove machined in the middle of the thick rib to generate two thin ribs. These operations could conveniently be conducted on the spinning machine setup itself or, alternatively, in a separate machining station requiring:

10 min/part for trimming both ends
20 min/part for rib undercutting

for a total of 0.5 standard hours per subshell with a one-man crew. Thus, the earlier estimate of 1 standard hour per subshell is well within the manpower capacity for this operation.

7.3.4 Inspection Station

The in-plant inspection tasks would consist of:

Dimensional test:	10 min/part
Hardness test:	10 min/part
Ultrasonic test:	10 min/part
X-ray test:	20 min/part
All others:	10 min/part

Inspection of the subshells thus accounts for one standard hour per subshell, as estimated previously.

7.4 SUBSHELL PRODUCTION COST OF INTERNAL SHEAR FORGING vs. CURRENT PROCESS

The labor requirement for internal shear forging of 2014 aluminum subshells with thermomechanical treatment has been estimated at 12 standard hours per part, whereas the current process of fabricating the subshell as a welded structure was estimated to consume 130 standard hours per part.⁴¹ The production costs derived from these figures show that shear forged subshells would cost about one-eighth the cost of a comparable fabricated structure.

The production costs for internal shear forging and the current process are estimated below, along with the projected annual return on investment and payback period from the \$1 million cost of implementing the new technology in production.

7.4.1 Production Cost--Internal Shear Forging

Direct labor (\$8/hr x 12 hr/part x 2000 parts)	\$192,000
Manufacturing overhead (175% of direct labor)	336,000
Raw material (\$3/lb x 10 lb/part x 2000 parts)	60,000
Tooling (including rework and replacement parts)	100,000
Consumables (lubricants, cutting tools, and supplies)	10,000
G&A, profit, etc. (35% of above costs)	<u>244,300</u>
Total cost of 2000 shear forged subshells	\$942,300
Cost per subshell	471.15

7.4.2 Production Cost--Current Process

Direct labor (\$8/hr x 130 hr/part x 2000 parts)	\$2,080,000
Manufacturing overhead (175% of direct labor)	3,640,000
Raw material (\$3/lb x 4 lb/part x 2000 parts)	30,000
Tooling (welding fixtures)	20,000
Consumables (electrodes, cutting tools, and supplies)	10,000
G&A, profit, etc. (35% of above costs)	<u>2,023,000</u>
Total cost of 2000 fabricated subshells	\$7,803,000
Cost per subshell	3,901.50

7.4.3 Return on Investment and Payback Period

The anticipated savings in producing 2000 subshells by internal shear forging, as opposed to current fabrication, is \$6,860,700. Since the 2000 parts would represent one year's production, the return on investment on the \$1,000,000 invested in new equipment and facilities would be \$6.86 in the first year on each dollar invested.

The payback period for the investment would be 1.7 months corresponding to the production of 392 subshells by the new method.

8. CONCLUSIONS AND RECOMMENDATIONS

Using shear forging tooling in conjunction with an engine lathe, internal shear forging experiments were conducted to establish procedures for producing missile primary structures as monolithic construction with integral ribs. This Manufacturing Methods and Technology Program successfully established guidelines for large-volume production of these structures and showed the cost savings resulting from implementation of the internal shear forging processes.

The major conclusions from this program are that:

- Internal shear forging can be implemented to produce missile primary structures to near-net shape.
- The cost savings accompanying implementation of this process are substantial.
- Although the strengthening effect of thermomechanical treatment seems to be minimal for 2014 aluminum on the basis of tensile data, further testing for fatigue, fracture, and stress corrosion resistance is necessary before the effects of TMT can be confirmed.
- Dimensional stability and residual stresses resulting from TMT must be fully characterized.

Before this cost-effective, near net shape technology is implemented, however, it is recommended that the thermomechanical aspects of the process be carefully reviewed and evaluated, in terms of the following:

- trade-off between higher property levels (if existent) and increased processing cost due to multiplicity of steps,
- influence of process variables on the reproductivity of end properties and product appearance,
- magnitude, polarity, and distribution of residual stresses resulting from TMT and their effect on the dimensions and mechanical properties of shear forged subshells.

REFERENCES

1. C. L. Packham, "Metal Spinning and Shear and Flow Forming," *Metallurgia and Metal Forming*, June 1976, pp. 168-70; July 1976, pp. 203-206; August 1976, pp. 250-252; September 1976, pp. 281-285.
2. C. Wick, "Metal Spinning: A Review and Update," *Manufacturing Engineering*, January 1978, pp. 73-77.
3. *Metal Deformation Processing, Vol. II*, Defense Metals Information Center, Battelle Memorial Institute, Columbus, Ohio, Report No. 226, 1966, pp. 49-66.
4. *Rotary Metalworking Processes*, Proceedings, First Int. Conf., IFS (Conferences) Ltd., Bedford, U.K., 1979.
5. K. W. Stalker and K. W. Moore, "Cold Power Spinning Saves Material, Cuts Costs," *American Machinist*, May 9, 1955.
6. "Power Spinning Conical and Tubular Parts," *Product Engineering*, August, 1956.
7. J. Genis and W. Mallindine, "Rotary Extrusion Reduces Costs and Saves Material," *Machinery (NY)*, April 1958, pp. 115-121.
8. J. H. Peters, "Flow Turning to Increase Strength, Save Weight, and Reduce Costs," ASME Paper No. 59-A-277, 1959.
9. L. E. Zwissler, "Spinning Makes Stronger Rocket Cases," *Metal Progress*, December 1960.
10. "Heavy Flow-Forming," *Aircraft Production*, November 1962, pp. 374-376.
11. D. J. Campion, "Spinning and Related Forming Techniques with Particular Reference to Maraging Steel," *Sheet Metal Industries*, March 1967, pp. 160-166.
12. G. E. Gott, J. M. Lynch, and S. M. Jacobs, "Are Shear Spinning and Roll Extrusion Production Processes for Large Parts?" *Metal Progress*, March 1968, pp. 95-99.
13. "Case Histories Demonstrate Metal Spinning's Virtues," *Modern Metals*, June 1978, pp. 46-49.
14. D. H. Pollitt, "The Practice and Potential of Flow Forming Processes," in *Rotary Metalworking Processes*, Proceedings, First Int. Conf., IFS (Conferences) Ltd., Bedford, U.K., 1979.
15. "Shear Forming of Thin-Wall Seamless Tubes," *Machinery*, January 1964, pp. 120-121.

16. A. W. Ernestus, "Roll Extrusion, A New Metal-Forming Technique," *American Machinist*, June 29, 1959, pp. 84-86.
17. D. L. Corn, "Roll Extruding Precision Seamless Pipe and Tubing," *Metal Progress*, June 1977, pp. 28-31. See also "Recent Advances in Roll Extrusion," in *Rotary Metalworking Processes, Proceedings, First Int. Conf.*, IFS (Conferences) Ltd., Bedford, U.K., 1979, pp. 243-250.
18. J. M. Steichen and R. L. Knecht, "Mechanical Properties of Roll Extruded Nuclear Reactor Piping," *ASME Paper No. 75-PVP-41*, 1975.
19. "Shear Forming: How It Affects Properties," *American Machinist*, July 6, 1965, pp. 57-59.
20. E. S. Jones, "Aus-Shear Forming of Low Alloy Steel Cylinders," General Electric Co., Cincinnati, Ohio, ca. 1960.
21. S. Kalpakjian, "An Application of Theory to an Engineering Problem: Power Spinning," in *Fundamentals of Deformation Processing*, Syracuse University Press, 1964, Chapter IV, pp. 71-103.
22. E. Thomasett, "Kräfte und Grenzformänderungen beim Abstreckdrücken zylindrischer, rotationssymmetrisches Hohlkörper aus Aluminium," Doctoral Dissertation, University of Stuttgart, 1961.
23. S. Kalpakjian, "An Experimental Study of Plastic Deformation in Power Spinning," *C.I.R.P. Annalen*, Vol. 10, 1962, pp. 58-64.
24. H. Jacob, "Erfahrungen beim Fliessdrücken zylindrischer Werkstücke," *Fertigungstechnik und Betrieb*, Vol. 12, March 1962, pp. 169-178.
25. E. Siebel and K. A. Dröge, "Forces and Material Flow in Spinning," *Werkstattstechnik und Maschinenbau*, Vol. 45, January 1955, pp. 6-9. (See also *The Engineers' Digest*, Vol. 16, No. 5, May 1955, pp. 193-195.)
26. S. Kalpakjian, "Maximum Reduction in Power Spinning of Tubes," *Trans. ASME, J. Eng. Ind.*, Vol. 86, 1964, pp. 49-54.
27. C. H. Wells, "The Control of Buildup and Diametral Growth in Shear Forming," *Trans. ASME, J. Eng. Ind.*, Vol. 90, 1968, pp. 63-70.
28. H. J. Dreikandt, "Untersuchung über das Drückwalzen zylindrischer Hohlkörper und Beitrag zur Berechnung der gedrückten Fläche und der Kräfte," University of Stuttgart, 1973.
29. S. Kalpakjian, "Chevron Fracture in Tube Reduction by Spinning," in *Advances in Research on the Strength and Fracture of Materials*, Vol. 2A, Pergamon Press, NY, 1977.

30. A. K. Cruden, Report No. 341, National Engineering Laboratory, 1968; also M. G. Cockcroft in *Ductility*, ASM, 1968, p. 218.
31. M. Hayama and H. Kudo, "Analysis of Diametral Growth and Working Forces in Tube Spinning," *Bulletin of the Japan Society of Mechanical Engineers*, Vol. 22, 1979, pp. 776-784.
32. M. Hayama and H. Kudo, "Experimental Study of Tube Spinning," *Bulletin of the Japan Society of Mechanical Engineers*, Vol. 22, 1979, pp. 769-775.
33. H. Jacob and F. Garreis, "Rollenanordnung und Rollenform beim Fliessdrücken kreiszylindrischer Körper," *Fertigungstechnik und Betrieb*, Vol. 15, No. 5, May 1965, pp. 279-283.
34. H. Jacob and F. Garreis, "Berechnung der auftretenden Kräfte beim Fliessdrücken zylindrischer Hohlkörper," *Fertigungstechnik und Betrieb*, Vol. 14, No. 8, August 1964, pp. 493-497.
35. H. Jacob and F. Garreis, "Fliessdrücken mit Schrägstellung der Rollen und deren Auswirkung und den Werkstofffluss und Umformkräfte (Dreh-Umformmaschine)," *Fertigungstechnik und Betrieb*, Vol. 16, No. 1, January 1966, pp. 42-45.
36. V. I. Eliseev and E. I. Isachenkov, "Selection of Force Parameters When Flow-Turning Cylindrical Components," *Russian Engineering Journal* (Translation of *Vestnik Mashinostroyenia*), Vol. 49, No. 11, 1969, pp. 68-71.
37. P. Bennich, "Tube Spinning," *Int. Journal Prod. Res.*, Vol. 14, No. 1, 1976, pp. 11-21.
38. J. A. Bennaton and E. Appleton, "An Experimental Metalforming Machine and Its Application to Cylindrical Flowturning," *Rotary Metalworking Processes*, Ref. 4.
39. T. Rammohan and R. Mishra, "Studies on Power Spinning of Tubes," *Int. Journal Prod. Res.*, Vol. 10, No. 4, 1972, pp. 351-364.
40. M. Azrin, G. B. Olson, E. B. Kula, and W. F. Marley, Jr., "Soviet Progress in Thermomechanical Treatment of Metals," *J. Appl. Metalworking*, Vol. 1, No. 2, 1980, pp. 5-34.
41. J. Long, MIRADCOM, private communication, 28 January 1981.

DISTRIBUTION LIST
(DAAK40-78-C-0264)

	<u>No. of Copies</u>
Commander US Army Missile Command ATTN: DRSMI-RLM Redstone Arsenal, AL 35809	10
Commander US Army Missile Command ATTN: DRDMI-EAT Redstone Arsenal, AL 35809	12 + camera-ready master
Commander US Army Missile Command ATTN: ACO Redstone Arsenal, AL 35809	1
Commander US Army Missile Command ATTN: PCO Redstone Arsenal, AL 35809	1
Defense Documentation Center Cameron Station Alexandria, VA 22314	2
Director Army Materials and Mechanics Research Center ATTN: DRXMR-PT Watertown, MA 02172	2
Director US Army Industrial Base Engineering Activity ATTN: DRXIB-MT Rock Island Arsenal Rock Island, IL 61201	2
Commander US Army Materiel Development & Readiness Command ATTN: DRCMT 5001 Eisenhower Avenue Alexandria, VA 22333	1

	<u>No. of Copies</u>
Commander US Army Tank-Automotive R&D Command ATTN: DRDTA-R Warren, MI 48090	1
Commander Frankford Arsenal ATTN: SARFA-MTT Bridge & Tacony Streets Philadelphia, PA 19137	1
Commander Picatinny Arsenal ATTN: SARPA-MT-C Dover, NJ 07801	1
Commander US Army Aviation Systems R&D Command ATTN: DRDAV-EXT 12th and Spruce Street St. Louis, MO 63166	1
Commander US Army Electronics R&D Command ATTN: DELET-TL-IC Ft. Monmouth, NJ	1
Commander US Air Force Materials Laboratory ATTN: AFML/LT Wright-Patterson Air Force Base Dayton, OH 45433	1
Commander Naval Materiel Command (Code 042) CP #5 Room 722 Washington, DC 20360	1